

Medical University Vienna

Institute for Cancer Research,
Applied and Experimental Oncology
Vienna, Austria

**Association between mutational background and response
to CDK4/6 inhibitors in human mesothelioma models.**

Bachelor thesis

University of Veterinary Medicine, Vienna

submitted by

Leah Mager

Vienna, July 2021

External supervisor:

Prof. Dr. Walter Berger,
Institute for Cancer Research,
Medical University of Vienna

Internal supervisor:

Prof. Dr. Florian Grebien,
Institute for Medical Biochemistry,
Veterinary University Vienna

Reviewer:

Dr. Mag^a rer.nat. Karoline Kollmann,
Institute for Pharmacology and Toxicology,
Veterinary University Vienna

Acknowledgements:

At first, I want to thank my external supervisor Prof. Dr. Walter Berger for his support and guiding and for giving me the great opportunity to write this bachelor thesis at his group where I had the chance to deal with this exciting topic and could gain priceless experience.

A special thanks goes to Dr. Lisa Mayr for her amazing support and guiding throughout the whole time at the institute, her valuable proofreading of my texts, her permanent helpfulness and especially for her patience and knowledge to answer each of my 1000 questions.

Furthermore, I want to thank the whole Berger/Heffeter group as they were all the reason that I had such a great and exciting time at the Institute.

I am also very grateful to Prof. Dr. Florian Grebien for his interest in my thesis as he agreed to be my internal supervisor and his helpful suggestions. Further my thanks also go to Dr. Karoline Kollmann who agreed to review my work.

Last but not least, I would like to thank my family and friends for their support and proofreading.

Table of content

1 Introduction	1
1.1 Malignant pleural mesothelioma	1
1.2 <i>CDKN2A</i>	2
1.2 The cyclin D ₁ -CDK4/6-RB pathway.....	3
1.4 Inhibition of the Cyclin D ₁ -CDK4/6-RB pathway	6
1.5 Aim of this thesis	8
2 Material and methods	9
2.1 Cell culture	9
2.1.1 Cell lines.....	9
2.1.2 Cell cultivation	9
2.2 Drugs.....	9
2.3 Viability assay	10
2.4 Clonogenicity assays	11
2.5 Western blotting	12
2.6 Statistical analyses	17
3 Results	18
3.1 Effects of CDK4/6 inhibition on malignant pleural mesothelioma cells	18
3.1.1 Short-term toxicity	18
3.1.2 Long-term toxicity.....	24
3.3 Impact of CDK4/6 inhibitors on downstream signaling pathways in malignant pleural mesothelioma cells:.....	31
4 Discussion	33
4.1 Response to CDK4/6 inhibitors.....	33
4.2 CDK4/6 effects on protein expression	34
4.3 Mechanism of abemaciclib induced cell death.....	35
4.4 Possible resistance mechanisms	37
4.5 Conclusion and future perspectives.....	38
5 Summary	39
6 List of abbreviations	41
7 Bibliography	42
8 Tables	44
9 Figures	45

1 Introduction

1.1 Malignant pleural mesothelioma

Mesothelioma especially malignant mesothelioma is a rare tumor developing in serosal tissues like pleura und peritoneum. One of the most common types of malignant mesothelioma is malignant pleural mesothelioma (MPM) which is commonly associated with asbestos exposure. Although the asbestos usage has been significantly reduced the incidence is still increasing due to the long latency period of 30 to 50 years before tumor development. In addition to the increasing usage of asbestos in Brazil or Africa there are less stringent rules that will ensure that MPM will remain a serious problem throughout the world. MPM can be classified into three major histological subtypes: the epithelioid histotype which is the most common type and with better prognosis in comparison to the sarcomatoid and the biphasic histotype. (Cakiroglu et al., 2020)

Nonspecific symptoms like chest pain, weight loss or dyspnea (Berzenji & Van Schil, 2018) and difficult differentiation between reactive surface mesothelial proliferation and mesothelioma (Churg et al., 2020) complicate diagnosis of MPM. The approved first-line treatment for MPM is a systemic application of platinum-based chemotherapy (cisplatin) combined with an antifolate (pemetrexed). Sometimes chemotherapy is accompanied by cytoreductive surgery but the usage is limited to patients with early stage disease and good functional status (Bibby et al., 2016). Surgery in MPM is following two main approaches: the extrapleural pneumonectomy (EPP) where the tumor, the lung, the pleura, the diaphragm and the pericardium are removed en-bloc and pleurectomy/decortication (P/D) where the parietal and visceral pleura is removed in order to eliminate the tumor but the diaphragm and the pericardium remain. Due to the lower mortality rate and higher quality of life after P/D surgery compared to EPP, P/D is currently the more common practice. (Sayan et al., 2019) To follow a multimodal approach and to increase effectivity of the treatment, chemotherapy and cytoreductive surgery can be combined with radiotherapy or immunotherapy. Although there are a few treatment options, prognosis for MPM patients remains poor and the median overall survival is only 12-27 months for the epithelioid subtype and even worse for the sarcomatoid

and biphasic subtype (7-18 months) which emphasizes the need for more effective therapeutic strategies. (Berzenji & Van Schil, 2018)

Considering the genetic profile of MPM, it is obvious that loss of function alterations most frequently affects three genes: BRCA1-associated protein 1 (*BAP1*), cyclin-dependent kinase 2A (*CDKN2A*) and neurofibromatosis type 2 (*NF2*) (Cakiroglu & Senturk, 2020) *BAP1*, a tumor-suppressor, plays an important role in cell cycle control, repair of DNA damage, cell differentiation and proliferation and is altered in multiple aggressive tumors (Louie & Kurzrock, 2020). The *NF2* gene encodes for the tumor-suppressor protein moesin-ezrin-radixin-like protein (merlin) which is involved in cell motility, migration and inhibiting signal transduction of pathways that are important for tumor cell proliferation like the phosphoinositide 3-kinase (PI3K) pathway.

1.2 *CDKN2A*

CDKN2A is a tumor-suppressor gene and involved in the regulation of two important cell cycle pathways, the p53 and the RB1 pathway by encoding the tumor-suppressor proteins p14^{ARF} and p16^{INK4}. p14 builds a complex with MDM2 and consequently prevents inactivation of p53 ensuring that the cell cycle is arrested and possible DNA damage is repaired or apoptosis is induced. P16 inhibits CDK4/6, which stimulates cell proliferation, by binding to the Cyclin-D1-CDK4/6 complex and leads to cell cycle arrest by blocking the phosphorylation of retinoblastoma protein (RB) and therefore the releasing of transcription factor E2 factor (E2F). (Robertson & Jones, 1999)

As mentioned before homozygous deletion of *CDKN2A* is one of the most frequent chromosomal alterations in malignant pleural mesothelioma and appears in more than 50 % of cases. Previous studies showed that *CDKN2A* loss in MPM is associated with a poorer prognosis for patients and therefore may be a promising treatment target (Markowitz et al., 2020)

1.2 The cyclin D₁-CDK4/6-RB pathway

The cell cycle is divided into different phases, the G₁ phase in which the cell grows and synthesizes protein and RNA, the S phase in which the chromosomal DNA is replicated, the G₂ phase which serves to prepare for mitosis and the M phase in which mitosis and the actual cell division takes place (Kasten & Giordano, 1998). To check environmental conditions and possible damage to DNA as well as correct spindle attachment of the chromosomes, there are three different checkpoints in the cell cycle at the transitions between the phases. This control system ensures that the integrity of the DNA is maintained and no pathologically altered cells enter the cell cycle. (Pucci et al., 2000)

The first checkpoint is located between G₁ and S phase (G₁ checkpoint) and serves to validate the suitability of environmental conditions for cell division and to check for DNA damage. Before entering mitosis there is a checkpoint that controls whether the complete DNA has been replicated without defects (G₂ checkpoint). Finally, between metaphase and anaphase of mitosis (M checkpoint), it is checked whether all chromosomes are correctly attached to the mitotic spindle (Figure 1).

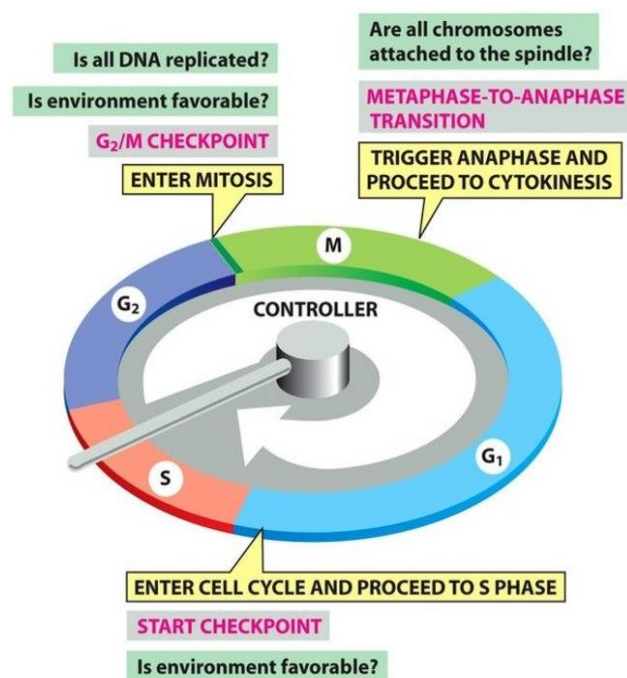


Figure 1: The control systems of the cell cycle (Alberts, 2017)

If the checkpoint detects a problem, the cell cycle is arrested by p53 or other tumor-suppressors and the damage is repaired or if it cannot be repaired apoptosis is induced. (Pucci et al, 2000)

The transition between the phases is regulated by cyclin dependent kinases and cyclins. Crucial for the transition of G₁ to S phase are the Cyclin-dependent kinases 4 and 6. CDK4/6 are serin/threonine kinases and are encoded by the CDK4 and the CDK6 gene. They are regulated by interactions with cyclins like cyclin D and CDK inhibitors like p16^{INK4} and play an important role on cell cycle progression by inducing G₁ phase to S phase progression. (Lim & Kaldis, 2013)

Proliferative stimuli like growth factors increase the expression of cyclin D₁ in the cell. Cyclin D forms a complex with CDK4/6 and ensures that the kinases become partially active (Studzinski & Danilenko, 2005). The CDK-activating kinase (CAK) phosphorylates the complex and makes it fully active (Figure 2).

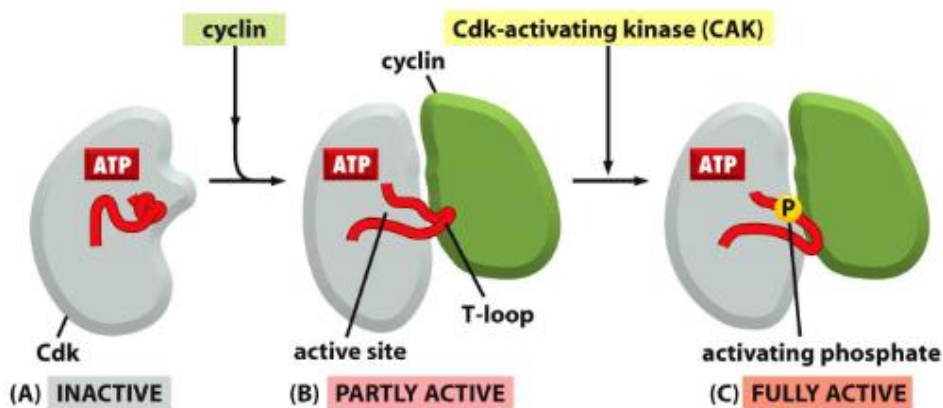


Figure 2: Activation of cyclin-dependent kinases (Alberts, 2017)

The active Cyclin D₁-CDK4/6-complex is transported to the nucleus where it phosphorylates the RB tumor-suppressor protein. In the active state, RB is hypophosphorylated and bound to the transcription factor E2F. This association blocks the ability of E2F to activate the transcription of certain genes that are required for S-phase initiation and DNA synthesis. Due to the phosphorylation of RB, E2F is released and is able to activate transcription of its target genes (Giacinti & Giordano, 2006). Furthermore, additional expression of cyclin E₁ is induced. Cyclin E₁ binds to CDK2 and subsequently RB is hyperphosphorylated followed by a further increased expression of E2F target genes which are essential for initiation of the S phase and DNA synthesis and cell cycle progression is induced (Figure 3). (Yuan et al., 2021)

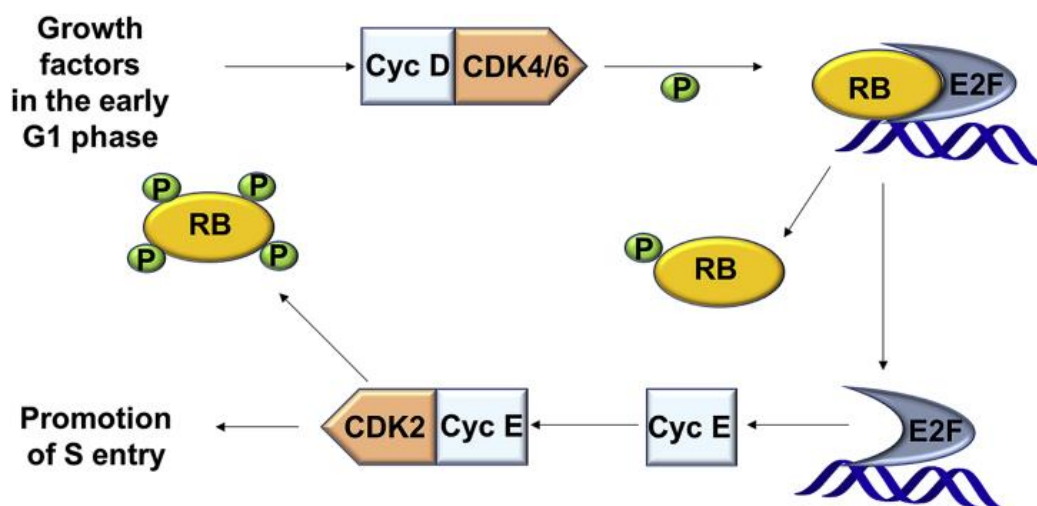


Figure 3: The Cyclin D- CDK4/6- RB pathway (Yuan et al., 2021)

In a variety of tumors, the Cyclin D₁-CDK4/6-RB pathway is dysregulated due to higher levels of Cyclin D₁ or increased activity of CDK4/6 caused by genomic or transcriptional aberrations like homozygous loss of *CDKN2A*. This dysregulation results in uncontrolled cell proliferation which is a pathological manifestation of cancer and therefore the Cyclin D₁-CDK4/6-RB and especially CDK4/6 are considered as a promising target for cancer treatment. (Vanarsdale et al., 2015)

1.4 Inhibition of the Cyclin D₁-CDK4/6-RB pathway

The tumor-suppressor protein p16 encoded by *CDKN2A* is able to inhibit the Cyclin D₁-CDK4/6- RB pathway and induces cell cycle arrest as it interferes complex formation between CDK and CDK6 cyclin D₁ by binding to the kinases. RB cannot be phosphorylated and remains bound to the transcription factor E2F and thus causes it to remain inactive (Figure 4). Unfortunately, p16 is often inactivated in a variety of cancers and in addition, cyclin D₁ is frequently overexpressed leading to the progression of the cell cycle and uncontrolled cell proliferation.

In consideration of this facts, a new promising generation of drugs has been developed to compensate the inactivation of p16 by inhibiting CDK4/6 and leading to cell cycle arrest in G₁ phase. (Figure 4)

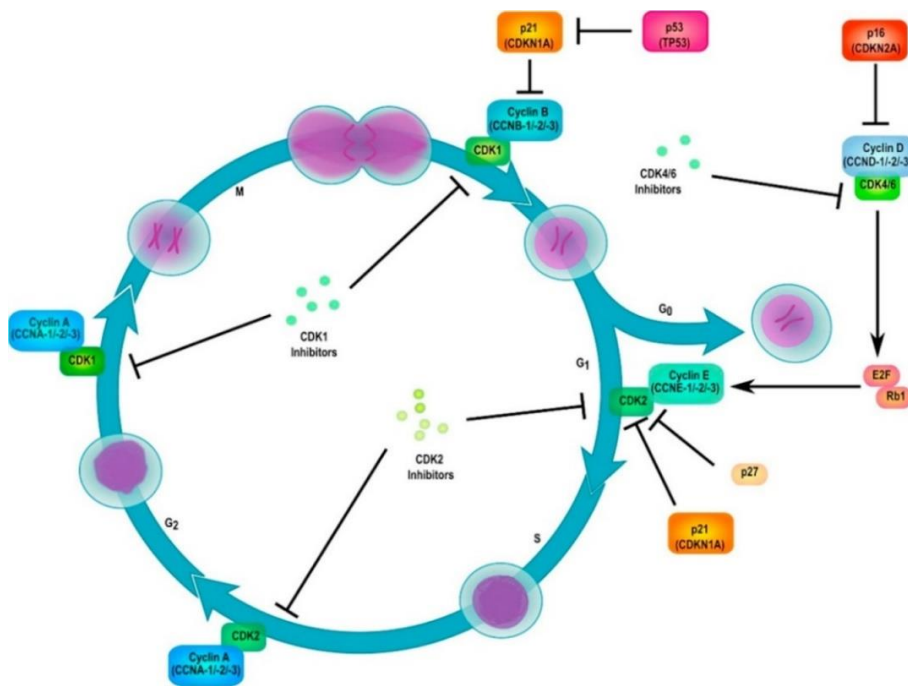


Figure 4: Inhibition of Cyclin D₁- CDK4/6- RB pathway and cell cycle progression by p16 and CDK4/6 inhibitors (Maner et al., 2020)

Abemaciclib, palbociclib and ribociclib (Figure 5) are approved for the treatment of advanced or metastatic hormone receptor-positive (HR+)/ human epidermal growth factor receptor 2 negative (HER2-) breast cancer in combination with specific endocrine therapies (aromatase inhibitor or fulvestrant) and selectively inhibit CDK4/6 with potent efficacy and reduced toxicity. (Ammazzalorso & Agamennone, 2021)

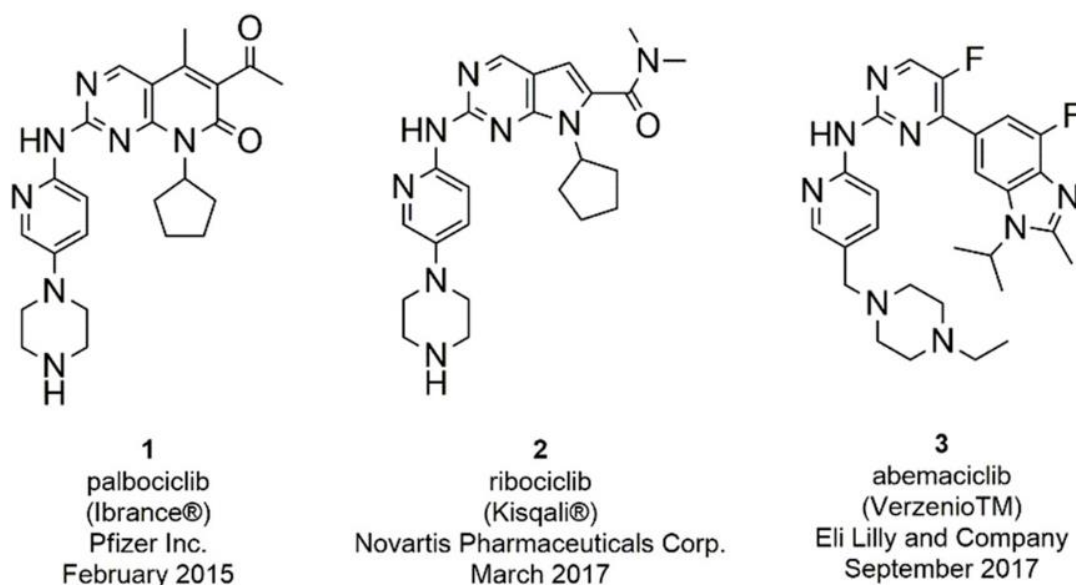


Figure 5: Structural formula abemaciclib, palbociclib and ribociclib (Ammazzalorso & Agamennone, 2021)

In addition to their good tolerability, clinical trials showed that they improved progression free survival in HR+/HER2- breast cancer in combination with an aromatase inhibitor (letrozole) for about 10 months in comparison to treatment only with letrozole. Hematologic toxicities, especially neutropenia are frequent side effects of palbociclib and ribociclib caused by the role of CDK6 in hematologic precursor proliferation. Due to its higher selectivity to CDK4, abemaciclib show lower rates of hematologic toxicity but indicates higher levels of gastrointestinal toxicity leading to diarrhea especially in the first time of treatment. But in general side effects are mild in most of the patients and are manageable with dose modifications. (Spring et al., 2019)

1.5 Aim of this thesis

Considering the increasing incidence of MPM and the poor prognosis for patients due to a lack of effective therapies, there is an utmost need for finding new targets and treatment strategies for malignant pleura mesothelioma.

Keeping in mind that the homozygous deletion of *CDKN2A* is one of the most common chromosomal alterations in MPM and is associated with worse survival it might be a promising therapy target. The inactivation of p16, caused by the deletion of *CDKN2A*, leads to the fact that CDK4/6 are no longer inhibited. This makes MPM with a homozygous loss of *CDKN2A* a promising candidate for the treatment with CDK4/6 inhibitors like abemaciclib, palbociclib and ribociclib.

This leads us to the working hypothesis that a homozygous *CDKN2A* loss in human mesothelioma cells may increase their sensibility for CDK4/6-inhibitors.

The aim of this thesis was to examine cytotoxic effects and the impact on protein expression of CDK4/6 inhibitors in human mesothelioma cell lines with different mutational background and to check whether they differ in the different cell lines.

2 Material and methods

2.1 Cell culture

2.1.1 Cell lines

To test the hypothesis, seven cell lines from malignant pleural mesothelioma with different genetic backgrounds were used. VMC 20 and VMC 46 had a normal expression of *CDKN2A*, Meso 110 and VMC 48 showed a mutation of *CDKN2A* and in VMC 23, Meso 49 and Meso 62 there was a homozygous deletion. The cell lines were established at the Medical University of Vienna from patient surgery samples and authenticated by short tandem repeat analyses. The age of the patients ranged from 42 to 86 years. With the exception of the cell line VMC 48, all patients were male. The tumors belonged to different histotypes, VMC 20, Meso 110 and VMC 23 were assigned to the epithelioid subtype, VMC 46, VMC 48 and Meso 49 to the biphasic and Meso 62 to the sarcomatoid subtype.

2.1.2 Cell cultivation

RPM1640 medium (Sigma-Aldrich, St. Louis, Missouri, USA) with 10 % fetal bovine serum (FBS, Gibco, Thermo Fisher Scientific, Waltham, Massachusetts, USA) was used for the cultivation of VMC 20, VMC 46, VMC 48 and VMC 23 cell lines. Meso 110, Meso 49 and Meso 62 cell lines were cultured with DMEM/F12 (Sigma-Aldrich, St. Louis, Missouri, USA) medium supplemented with 10% FBS. All cell lines were stored in a 5% CO₂ incubator at 37 °C.

2.2 Drugs

For drug treatment the CDK4/6- inhibitors abemaciclib, palbociclib and ribociclib (Selleck Chemicals Llc, Houston, Texas, USA) were used. All inhibitors were stored in powder form at -80 °C but for experiments, aliquots with a concentration of 10 mM per µl dissolved in Dimethyl Sulfoxide (DMSO) or H₂O, stored at -20 °C, were taken.

2.3 Viability assay

To check short term toxicity MTT assays were performed. To isolate cells for the experiment the complete medium in the cell culture flask was aspirated and few drops of trypsin EDTA were added. The cells were swirled in trypsin, then 1 ml of trypsin was added and incubated for a few minutes. In between, the cells were checked under the microscope to see if they had already detached. After the cells had detached from the bottom, the flask was rinsed with 1 ml medium. The cells were centrifuged 5 minutes at 1200 rpm and the supernatant was aspirated then. The remaining cell pellet was resuspended with medium. To determine cell number, 10 μ L cell suspension was mixed with 10 μ L of Trypan Blue (Sigma Chemical Company, St. Louis, Missouri, USA) and placed in a Neubauer counting chamber (Hecht Assistent, Sondheim, Germany) and then counted. Trypan blue was used to stain dead cells. A solution containing 3×10^4 or 4×10^4 cells per ml depending on the cell line was prepared based on the cell number. Cells were seeded in 96 well plates at a density of 3×10^3 or 4×10^3 cells per well. The plates were then incubated for 24 hours at 37 °C and 5% Co₂.

After 24 hours, the cells were treated with drugs of interest. In this case, these were abemaciclib, palbociclib and ribociclib. Dilutions of the drugs with the concentrations ranging from 0.5-10 μ M were prepared from a 10 mM stock. 100 μ l of the different concentrations were added in triplicates. The treated plates were incubated for 72 hours at 37 °C and 5% Co₂.

72 hours after treatment, short term toxicity was determined using a MTT viability assay. The Ez4u assay (Biomedica, Vienna, Austria) was used for this purpose. All medium was removed from the wells with the cells and 100 μ l of developer solution was added. In addition to this, solution was also added to 3 wells in which there were no cells, these served as reference values. The plates were placed for at least one hour in the incubator. After one hour, absorbance was measured at 450nm and a reference wavelength of 620 nm using Tecan infinite m200 Pro (Zurich, Switzerland). The plates were placed back in the incubator then and measured again after two hours.

In total, we conducted three assays per cell line

2.4 Clonogenicity assays

To examine long-term toxicity effects of the different inhibitors on cell growth clonogenicity assays were carried out. Cells were prepared as previously described for MTT and then seeded in triplicates in 24 well plates with a density of 1×10^3 to 5×10^3 per well depending on the cell line.

After incubation for 24 hours, either 500 μL of medium for the control wells or 500 μL of 0.5 μM abemaciclib, 1 μM palbociclib or 1 μM ribociclib was added to the cells. Triplicates were prepared per concentration.

After seven days of drug exposure the cells were either retreated or stained with crystal violet. For this, first the complete medium was removed and the cells were washed with cold phosphate buffered saline (PBS). Then cold methanol was added and the plates were placed in the refrigerator for 30 minutes. After 30 minutes the methanol was removed and cells were washed again with PBS. Afterwards cells were stained with crystal violet. The crystal violet was removed and the plates were washed with water, stroked and left to dry.

After drying, the colored cells were photographed and then converted to black and white. These photos were analyzed using ImageJ (Image J2, Wayne Rasband, NIH, Bethesda, Maryland, USA). A one-way analysis of variance (one-way ANOVA) was performed to find out whether the drugs had a significant effect on the cells compared to the control.

2.5 Western blotting

Effects on protein expression and downstream signaling of cells 24 hours after exposure to 1 μ M of the different drugs were studied using western blots. For western blotting, one ml of cell suspension containing 3×10^5 cells were seeded in 6 well plates, following the principle as described previously for MTT assays. When the cells were confluent, medium, 1 μ M abemaciclib, 1 μ M palbociclib or 1 μ M ribociclib were added.

One day after treatment, the proteins were isolated as follows. First, the cells were scratched in their medium on ice until they detach. Then washed with PBS and transferred to a centrifuge tube. Centrifugation at 1200 rpm for 10 minutes at 4 was followed by aspiration of the supernatant and resuspension of the pellet with one ml of PBS. Subsequently, the cells were centrifugated again. For pellet lysing lysis buffer (Table 1) with TritonX-100 supplemented with the protease inhibitors Phenylmethylsulfonyl fluoride (PMSF) and cOmplete™ and the protease inhibitor phospho-stop was added and incubated on ice for one hour and additionally mechanically lysed by pipetting up and down. The samples were then placed in an ultrasonic bath for 5 minutes and centrifuged at 14800 rpm at 4 degrees for 15 minutes. 2.5 μ L of the resulting supernatant was placed in an epi for protein determination, the remainder was frozen at -80 degrees until further use.

Lysis buffer:
50 mM Tris
300 mM NaCl
0.5 % TritonX-100

Table 1: Components Lysis buffer for protein extraction

Before western blotting protein concentration of the samples were determined by using Pierce™ BCA Protein Assay Kit (Thermo Fisher, Waltham, Massachusetts, USA). BSA standards with known concentrations were produced and pipetted into a 96 well plate. Protein samples were diluted in Aqua bidest (1:200) and also added to the plate. 150 μ l developing solution was added to the samples and the plate was incubated for at least two to three hours.

Absorbance could be measured at 560 nm by Tecan infinite m200 Pro. This reaction was based on the reduction of Cu^{2+} to Cu^{1+} by proteins (biuret reaction) followed by the reaction of bicinchoninic acid (BCA) with the reduced cuprous cation producing the color.

Initially, the 10 % polyacrylamide gel was prepared using distilled water, Acrylamide, Tris Hydrochloride (HCl, 1.5M; pH 8.8) and 20 % Sodium dodecyl sulfate (SDS). To start polymerization 10% Ammonium persulfate (APS) and Tetramethyl ethylenediamine (TEMED) were added. The mixture was filled into the western blot chamber covered with 70% ethanol to obtain a smooth surface and left about 20 minutes for polymerization.

After polymerization of the gel a 4.5% polyacrylamide gel has been prepared by mixing distilled water, Acrylamide, Tris HCl (1.5M; pH 8.8), 20 % SDS, 10% APS, and TEMED. The ethanol was removed from the separation gel and the collection gel was added into the western blot chamber on top of the separation gel. The comb was placed for the sample slots and the gel was left for at least 20 minutes for polymerization.

	10% separation gel	4.5 % collection gel
Distilled H ₂ O	3.65 ml	1.56 ml
Acrylamide	1.875 ml	0.281 ml
TrisHCl (1.5M; pH 8.8)	1.875 ml	0.625 ml
20% SDS	75 μ l	25 μ l
10% APS	25 μ l	12.5 μ l
TEMED	5 μ l	2.5 μ l

Table 2: Components polyacrylamide gels

Based on the previously determined concentration, the protein samples were dissolved with Lysis buffer and 15 μ l of this solution was mixed with 5 μ l 4x loading buffer to obtain a protein content of 15 μ g per sample.

	4x sample loading buffer
99,5% Glycerin	4 ml
2-Mercaptoethanol	2 ml
SDS	0.92 g
Bromophenol blue	0.2 mg
1M Tris-HCl (pH 6.8)	2.5 ml
Aqua bidest	bring on 10 ml

Table 3: Components sample loading buffer

Subsequently to the polymerization of collection gel the western blot chamber was placed into the electrophoresis chamber and filled up with 1 x Lämmli-Electrophoresis buffer. The sample slots were rinsed with the buffer then the samples and the marker (Precision Plus Protein™ Standard, BIO-RAD, Hercules, California, USA) were loaded into the gel slots and electrophoresis at 90V for one to two hours was started.

	10x Lämmli-Electrophoresis buffer
Tris	30 g
Glycine	144 g
Methanol	200 ml
Aqua bidest	bring on 1l

Table 4: Components running buffer

After electrophoresis finished the gels were washed for five minutes in Bjerrum buffer with SDS. For semidry-blotting a polyvinylidenfluorid (PVDF) membrane and two filter papers were used. The membrane was activated in methanol then transferred to Bjerrum buffer with methanol. One filter paper was placed to Bjerrum buffer with methanol. The other one to Bjerrum buffer with SDS. The filter in Bjerrum buffer with methanol followed by the activated membrane the gel and the filter with Bjerrum buffer with SDS were stacked in this order into the semidry-blotting machine (Trans-Blot Turbo Transfer System, BIORAD, Hercules, California, USA). Semidry-blotting was performed at 0.8 mA per blot for 30 minutes.

	Bjerrum buffer	+Methanol	+SDS
Tris	5.82 g		
Glycine	2.93 g		
Methanol		200 ml	
SDS			0.375 g
Aqua bidest	bring on 1l		

Table 5: Components Bjerrum buffer

Following blotting, the membrane was washed with ddH₂O and then stained with ponceau red to check whether the blotting worked. To remove the staining solution, the blots were washed with Aqua bidest and 1x Tris-buffered saline with Tween20 (TBST). Non-specific binding sites were blocked by incubating the membrane for one hour in a solution containing 10 ml 1x TBST with 5 % milk powder per blot. Before the blot was incubated overnight at 4 degrees under constant agitation with the primary antibody, it was washed three times with TBST. Each wash step with TBST was performed for at least 10 minutes with constant panning at the belly dancer (Stovall Life Science Inc, Greensboro, North Carolina, USA) All primary antibodies were diluted in 3 % BSA in 10 ml 1x TBST.

	1xTBST
10xTBS, pH:7.6 (120g TRIS, 90gNaCl, dissolved in 1l H ₂ O)	100 ml
Aqua bidest	900 ml
Tween	1 ml

Table 6: Components 1xTBST washing solution

Primary Antibody	Source	Secondary Antibody
RB	Santa Cruz	Mouse
pRB (Ser807/811)	Cell Signaling	Rabbit
Cyclin D1	Cell Signaling	Rabbit
Cyclin E1	Cell Signaling	Mouse
CDK4	Cell Signaling	Rabbit
CDK6	Cell Signaling	Mouse
S6	Santa Cruz	Rabbit
pS6 (Ser240/244)	Cell Signaling	Mouse
AKT	Cell Signaling	Rabbit
pAKT (Ser473)	Cell Signaling	Rabbit
ERK 44/42	Cell Signaling	Rabbit
pERK 44/42	Cell Signaling	Rabbit
β -Actin	Sigma Aldrich	Rabbit

Table 7: Primary antibodies for western blotting

The following day, the primary antibody was removed and the blots were washed again three times with TBST. The washing steps were followed by the addition of the appropriate secondary antibodies linked with horseradish peroxidase in 1 % BSA in 10 ml 1x TBST per blot for one hour. Another three washing steps afterwards, the peroxidase signal was detected by using chemiluminescence detection. Two ml of a luminol solution and 0.6 μ l hydrogen

peroxide (Sigma-Aldrich) per blot were used as substrates for chemiluminescence. Signals were then captured on x-ray films (Amersham Hyperfilm™ ECL, GE Healthcare limited, Chicago, Illinois, USA) and developed with the X-ray film processor (OPTIMAX2010, Protec, Oberstenfeld, Germany) The blots were washed again three times with 1xTBST and then incubated again overnight with another primary antibody or inactivated with methanol and dried until further use. β -actin served as a loading control.

	Luminol solution
TrisHCL (1M, pH: 8.8)	5 ml
3-Aminophthalhydrazide	250 μ l
Coumaric acid	125 μ L
Aqua bidest	bring on 50 ml

Table 8: Luminol solution for western blotting

2.6 Statistical analyses

To visualize and analyze the raw data and to test for statistical significance GraphPad Prism 8.0.1 (GraphPad Software Inc., La Jolla, California, USA) was used. Mean values +/- standard deviation (SD) of the measured absorbance values of cell viability assays were determined and normalized. Based on the normalized data IC₅₀ values (the concentration of the drug required to reduce cell viability by 50%) were calculated if they are not exceeding ten. Average IC₅₀ values were displayed with calculated standard error of the mean. To evaluate if the drug treatment in the long-term toxicity assay had a significant effect on cell survival and cell growth a one- way ANOVA was performed. Calculated p-values of less than 0.05 were considered statistically significant. The p values were classified as follows: *, $p < 0.05$; **, $p < 0.01$ ***, $p < 0.001$, ****, $p < 0.0001$.

3 Results

3.1 Effects of CDK4/6 inhibition on malignant pleural mesothelioma cells

3.1.1 Short-term toxicity

In order to estimate short-term toxicity effects of abemaciclib, palbociclib and ribociclib on the different malignant pleural mesothelioma cell lines we performed MTT assays. Cells were treated with different concentrations of the CDK4/6 inhibitors (0-10 μ M) and cell viability was determined after 72 hours.

Based on the results of the MTT assays, it is clear that all cell lines respond mainly to abemaciclib. Since the IC₅₀ values for palbociclib and ribociclib were close to or above 10 μ M in most experiments, they could not be reliably determined in most of the cell lines. Therefore, only the mean values for abemaciclib are presented here. Table 9 shows the calculated average IC₅₀ values for abemaciclib. For each cell line, one graph is representatively shown.

Unfortunately, we could not perform MTT assays as well as the more sensitive ATP assay with the cell line VMC 46, because the reference values could not be reached by far despite an increased number of seeded cells.

Considering the average IC₅₀ values, it becomes clear that cell lines with a mutational background of *CDKN2A* (homozygous deletion or mutation) with IC₅₀ values from 0.9-2.1 μ M show a higher sensibility towards abemaciclib than the cells with a normal expression of *CDKN2A* with a IC₅₀ value of 3.7 μ M (Table 9).

CELL LINE	<i>CDKN2A</i>	IC ₅₀ MEAN	SEM
VMC 20	normal expression	3,7	0,625
VMC 48	mutation	1.0	0.226
MESO 110	mutation	0.9	0.200
VMC 23	homozygous deletion	0.9	0,116
MESO 49	homozygous deletion	0.9	0,252
MESO 62	homozygous deletion	2.1	0,208

Table 9: Average IC₅₀ values for abemaciclib after 72 hours drug exposure in concentration of 0 – 10 μ M

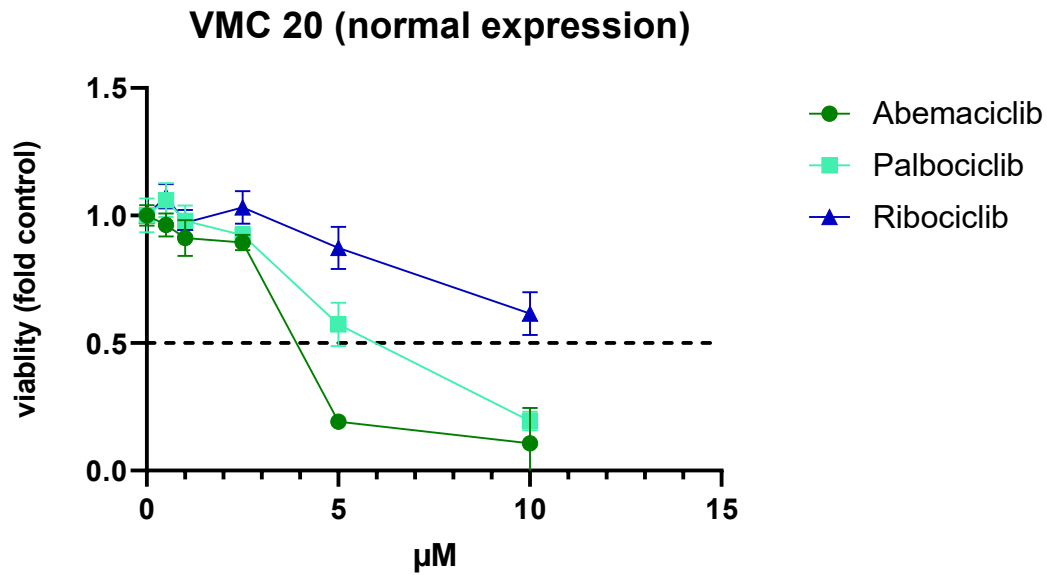


Figure 6: Effects of treatment with different CDK4/6 inhibitors in human mesothelioma cell line VMC 20 representatively shown for one experiment.

The impact of abemaciclib, palbociclib and ribociclib in concentration from 0-10 µM on cell viability is determined after 72 h of incubation with a MTT assay. Toxicity effect is shown as IC_{50} value. IC_{50} abemaciclib: 3.4 µM; IC_{50} palbociclib: 5.8 µM

Based on the performed MTT assays an average IC_{50} value of 3.7 µM (Table 9) for abemaciclib could be determined for VMC 20 with no alteration of *CDKN2A*. Compared to the other cell lines, this is a decreased sensitivity. Furthermore, VMC 20 showed response to palbociclib with an average IC_{50} value of 4.5 µM. Interestingly, this cell line showed more sensitivity when compared to the other tested cell lines. The IC_{50} value for ribociclib exceeded 10 µM and could not be determined. Figure 6 shows the effects on cell viability caused by the three CDK4/6 inhibitors in VMC 20 representatively for one performed experiment.

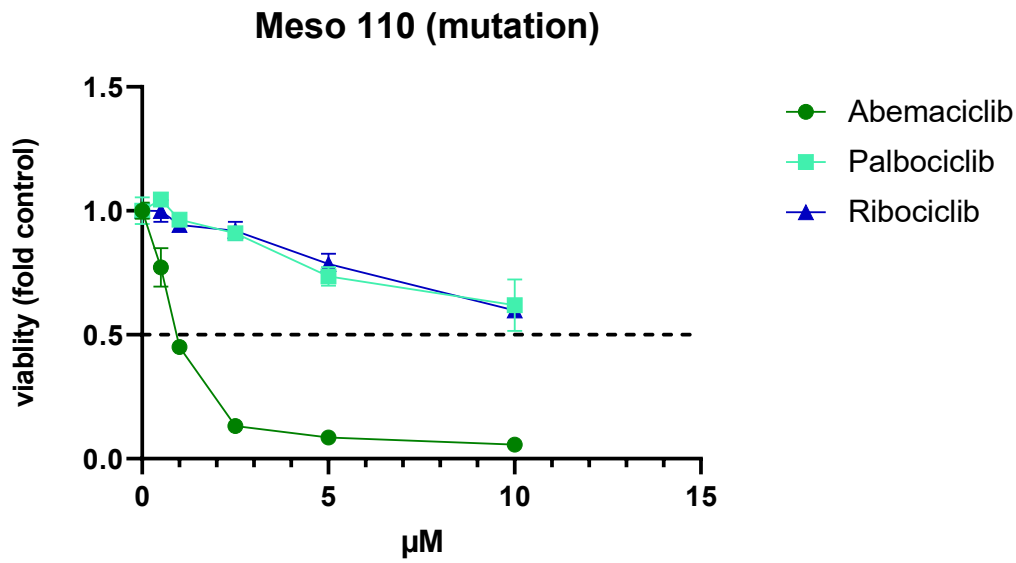


Figure 7: Effects of treatment with different CDK4/6 inhibitors in human mesothelioma cell line Meso 110 representatively shown for one experiment.

The impact of abemaciclib, palbociclib and ribociclib in concentration from 0-10 μM on cell viability is determined after 72 h of incubation with a MTT assay. Toxicity effect is shown as IC_{50} value. IC_{50} abemaciclib: 0.9 μM

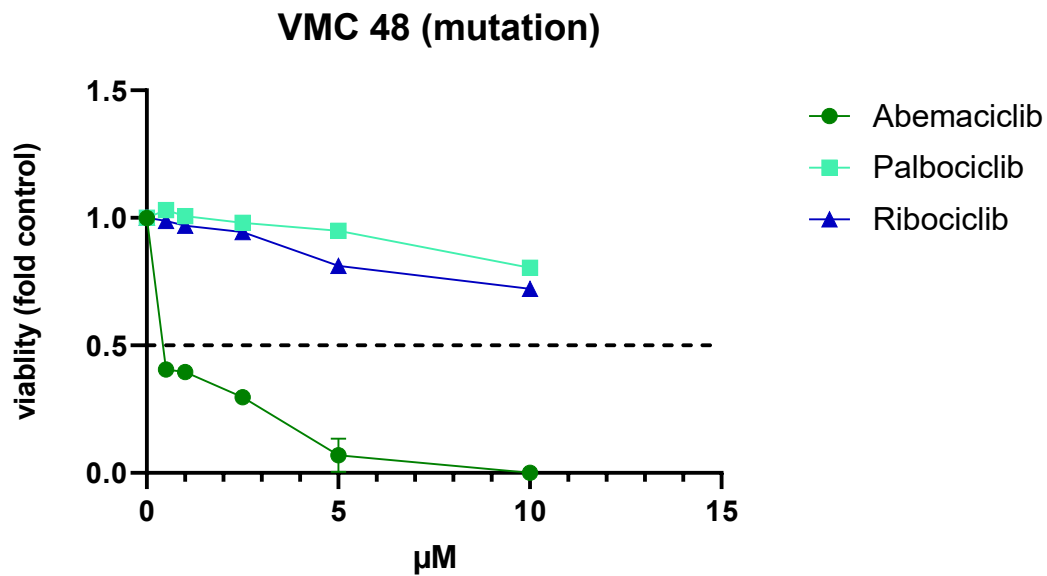


Figure 8: Effects of treatment with different CDK4/6 inhibitors in human mesothelioma cell line VMC 48 representatively shown for one experiment.

The impact of abemaciclib, palbociclib and ribociclib in concentration from 0-10 μM on cell viability is determined after 72 h of incubation with a MTT assay. Toxicity effect is shown as IC_{50} value. IC_{50} abemaciclib: 0.8 μM

Both cell lines with a *CDKN2A* mutation (VMC 48, Meso 110) showed distinct sensitivity to abemaciclib in short-term toxicity experiments. For VMC 48 a IC_{50} value of $1\mu M$ was determined (Table 9). For Meso 110, an average IC_{50} value of $0.9\mu M$ has been defined (Table 9). In both cell lines palbociclib and ribociclib achieved IC_{50} values exceeding $10\mu M$. The observed effects of all three CDK4/6 inhibitors on cells with a mutation of *CDKN2A* are illustrated in figures 7 and 8.

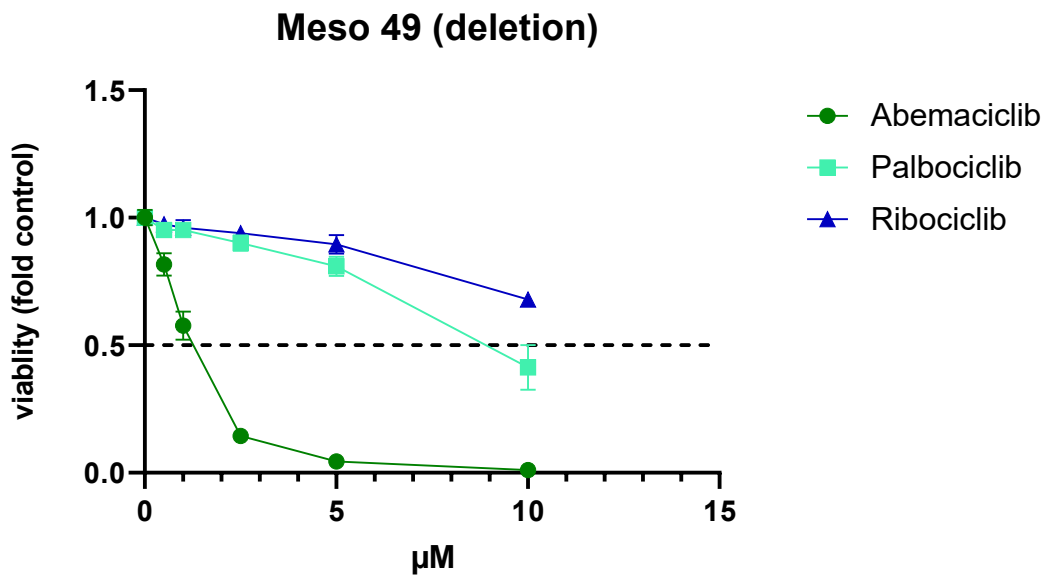


Figure 9: Effects of treatment with different CDK4/6 inhibitors in human mesothelioma cell line Meso 49 representatively shown for one experiment.

The impact of abemaciclib, palbociclib and ribociclib in concentration from 0-10 μM on cell viability is determined after 72 h of incubation with a MTT assay. Toxicity effect is shown as IC_{50} value. IC_{50} abemaciclib: $1.2\mu M$; IC_{50} palbociclib: $9.5\mu M$

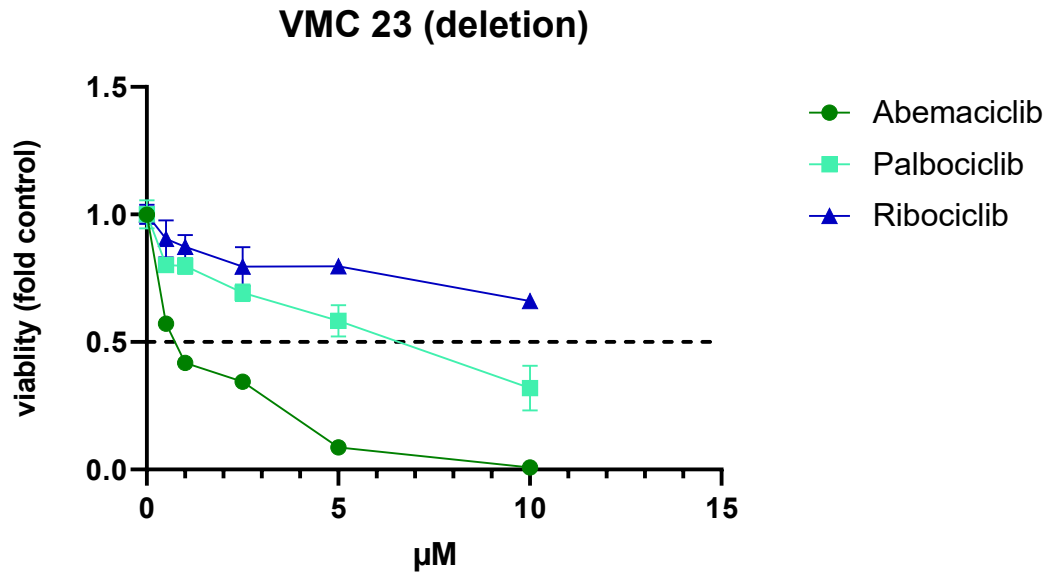


Figure 10: Effects of treatment with different CDK4/6 inhibitors in human mesothelioma cell line VMC 23 representatively shown for one experiment.

The impact of abemaciclib, palbociclib and ribociclib in concentration from 0-10 µM on cell viability is determined after 72 h of incubation with a MTT assay. Toxicity effect is shown as IC_{50} value. IC_{50} abemaciclib: 1.0 µM; IC_{50} palbociclib: 7.0 µM

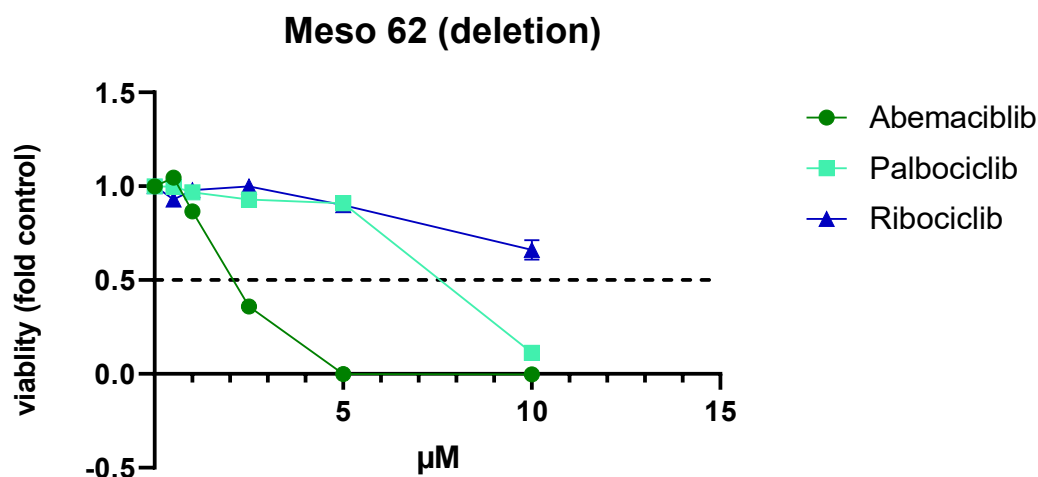


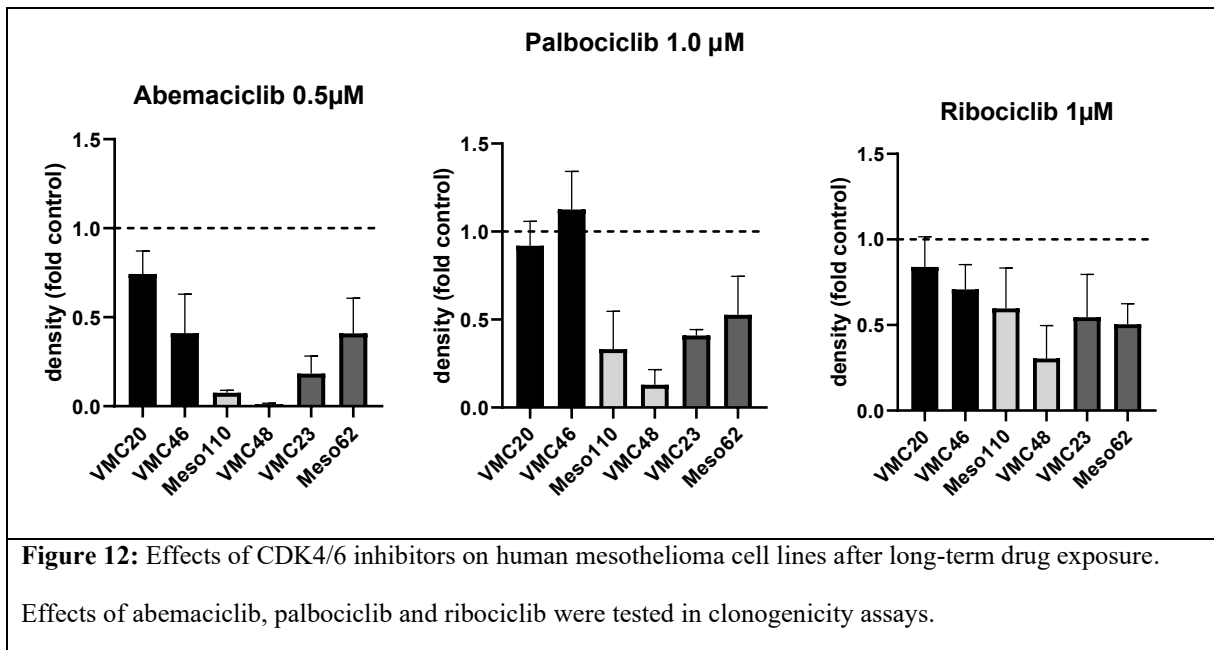
Figure 11: Effects of treatment with different CDK4/6 inhibitors in human mesothelioma cell line Meso 62 representatively shown for one experiment.

The impact of abemaciclib, palbociclib and ribociclib in concentration from 0-10 μM on cell viability is determined after 72 h of incubation with a MTT assay. Toxicity effect is shown as IC_{50} value. IC_{50} abemaciclib: 2.3 μM ; IC_{50} palbociclib: 8.0 μM

Looking at the short-term toxicity results of the cell lines with a homozygous deletion of *CDKN2A*, it is obvious that the cell line Meso 62 differed from the other two. While VMC 23 and Meso 49 only required an average drug concentration of 0.9 μM to reach IC_{50} , Meso 62 required an average drug concentration of 2.1 μM (Table 9). All three cell lines showed IC_{50} values of palbociclib. However, since these were either very high (VMC 23, 7.5 μM) or outside the detection limit (Meso 49 and Meso 62, exceeding 10 μM), they were not considered relevant. No IC_{50} values were reported for treatment with ribociclib. For visualization figures 9-11 show antiproliferative effects on the cells with a homozygous deletion of *CDKN2A* induced by abemaciclib, palbociclib and ribociclib. Representatively one experiment is depicted for each cell line.

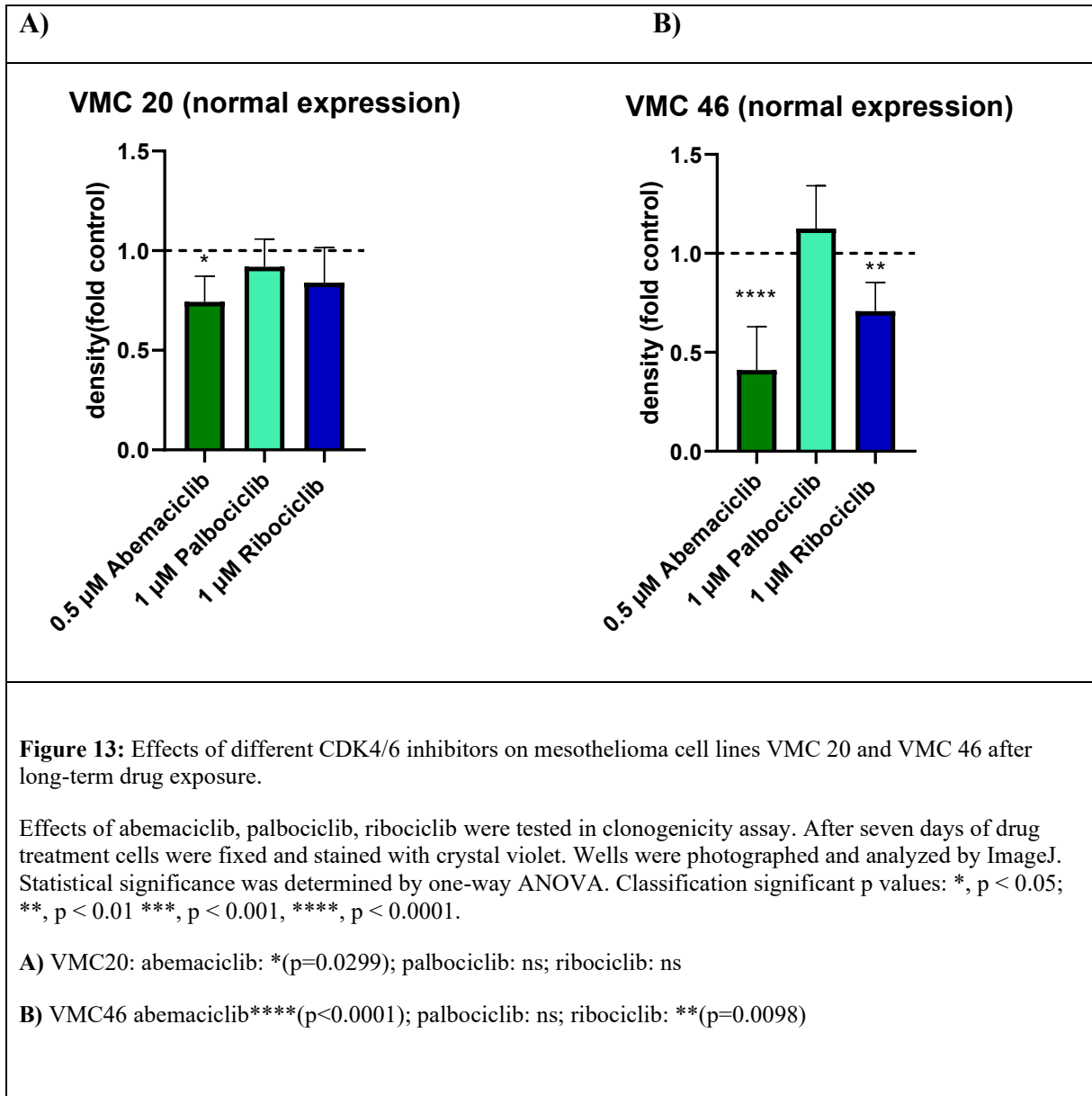
3.1.2 Long-term toxicity

To determine long-term toxicity effects on cell viability we performed clonogenicity assays. Unfortunately, Meso 49 (homozygous deletion) cells died after several days in culture and therefore were not suitable for further analysis.



Similarly, to the short-term toxicity assays, the most pronounced effects were seen with abemaciclib although it was only half as concentrated as palbociclib and ribociclib (0.5 µM, 1 µM, 1 µM respectively, Figure 12) as it was able to reduce cell viability significantly in all cell lines. However, palbociclib and ribociclib, in contrast to the MTT results, also achieved significant inhibitory effects on all cell lines with the exception of VMC20 (Figure 13). In general, the cell lines with a mutation of *CDKN2A* responded most effectively to all three treatments.

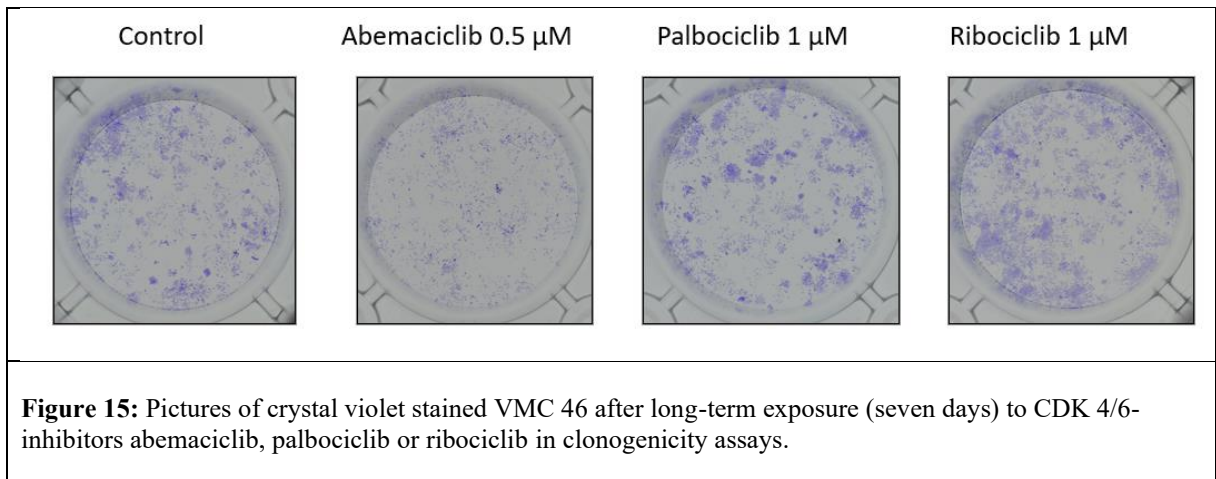
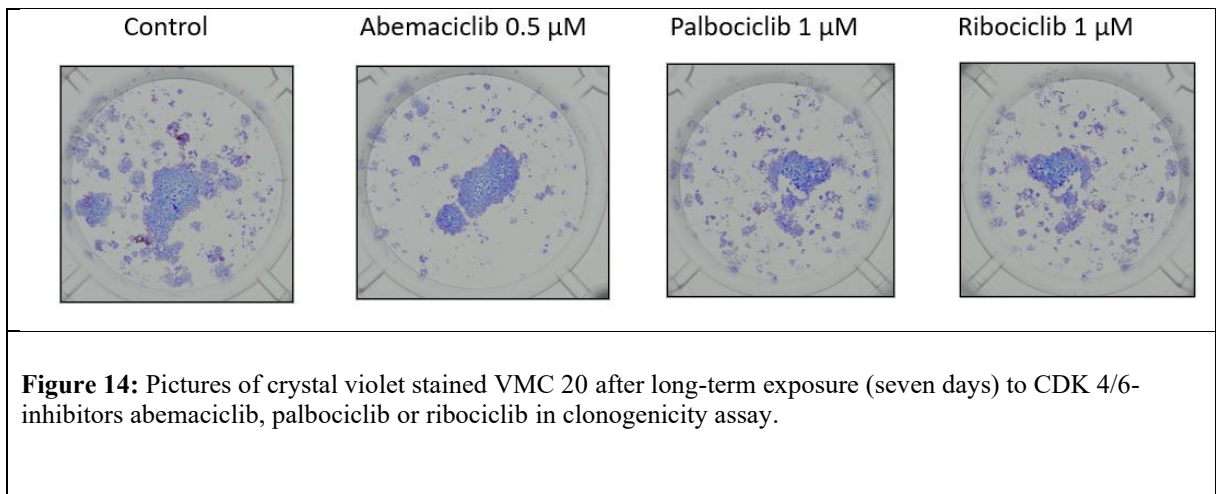
For all cell lines, the average inhibitory effects by all drugs used are shown below. Photos of crystal violet-stained cells are depicted.

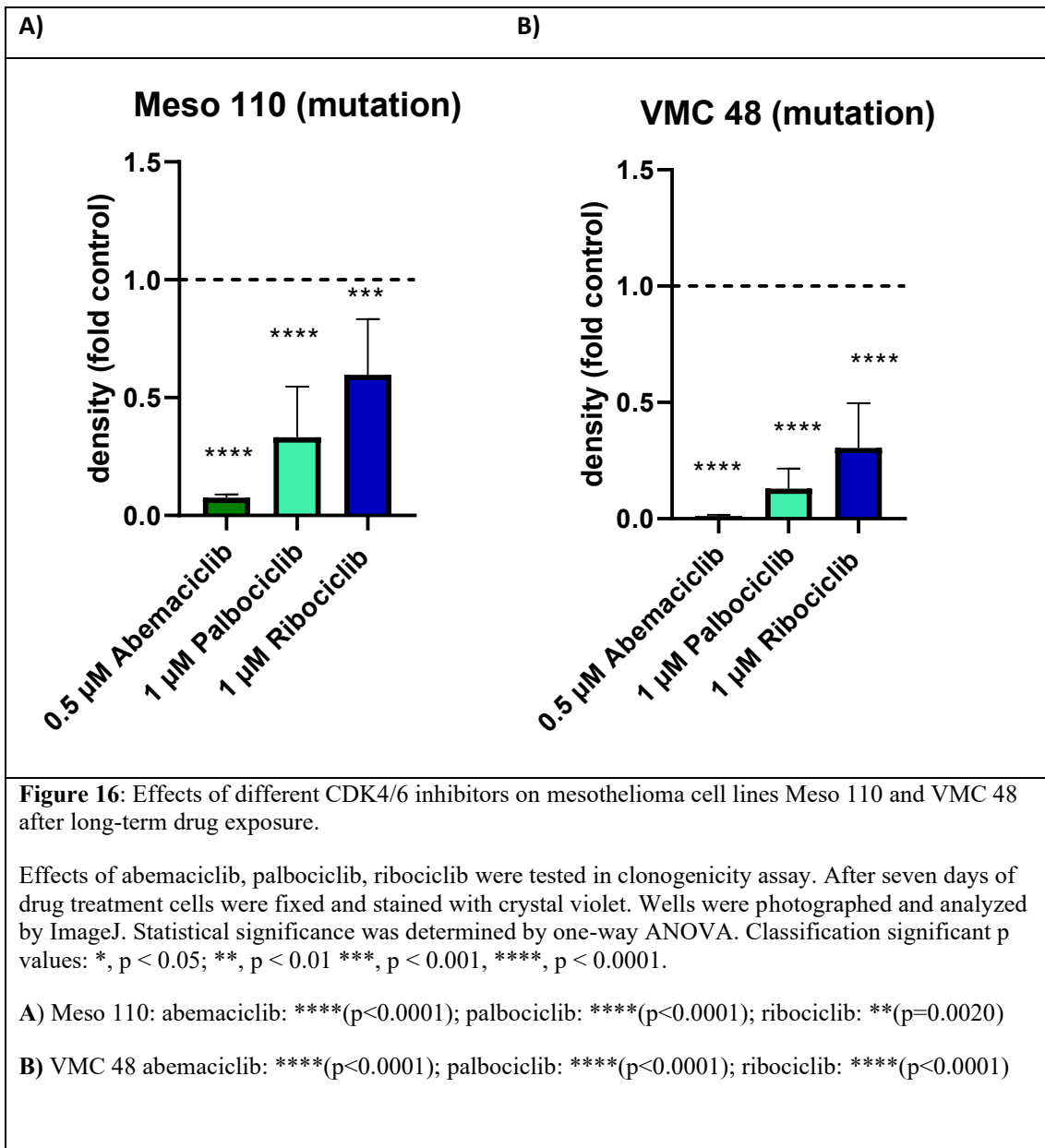


Considering the results of clonogenicity assays of VMC 20, only abemaciclib shows a detectable effect (Figure 13A, 14). However, compared to the other cell lines, this effect was

relatively small and reduced cell viability by about 25 percent. Interestingly, palbociclib showed no significant reduction of cell viability although cells responded in the MTT assays.

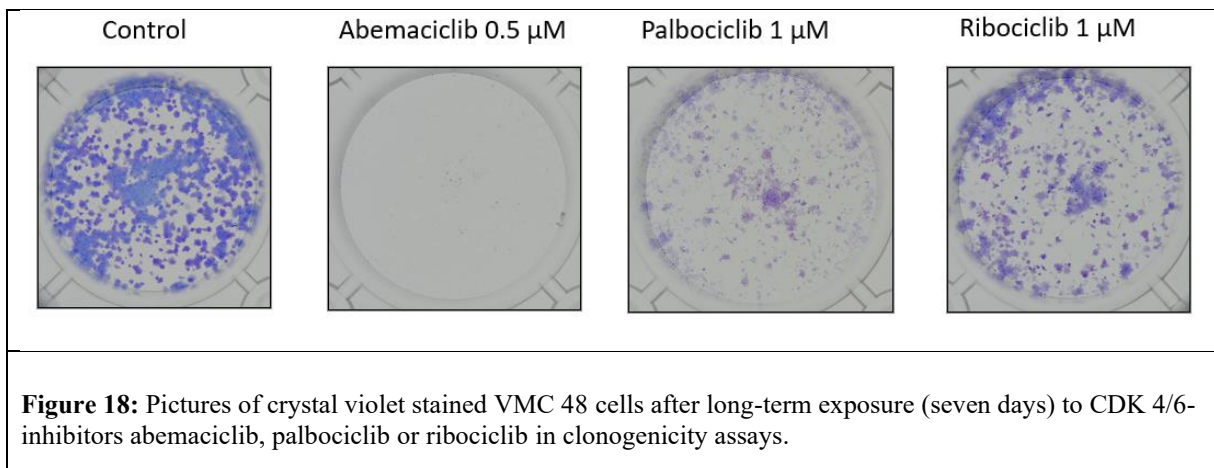
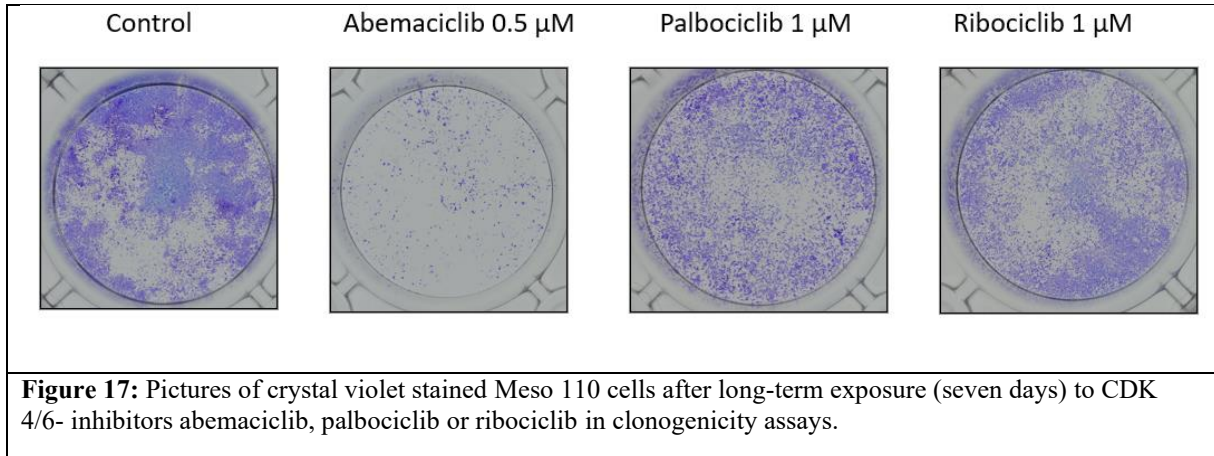
In contrast to the results of VMC 20, the inhibitory effects of abemaciclib in VMC 46 (Figure 13B, 15) were much more significant and the cell viability could be reduced by more than 50 %. Ribociclib also significantly reduced cell viability by approximately 40%.

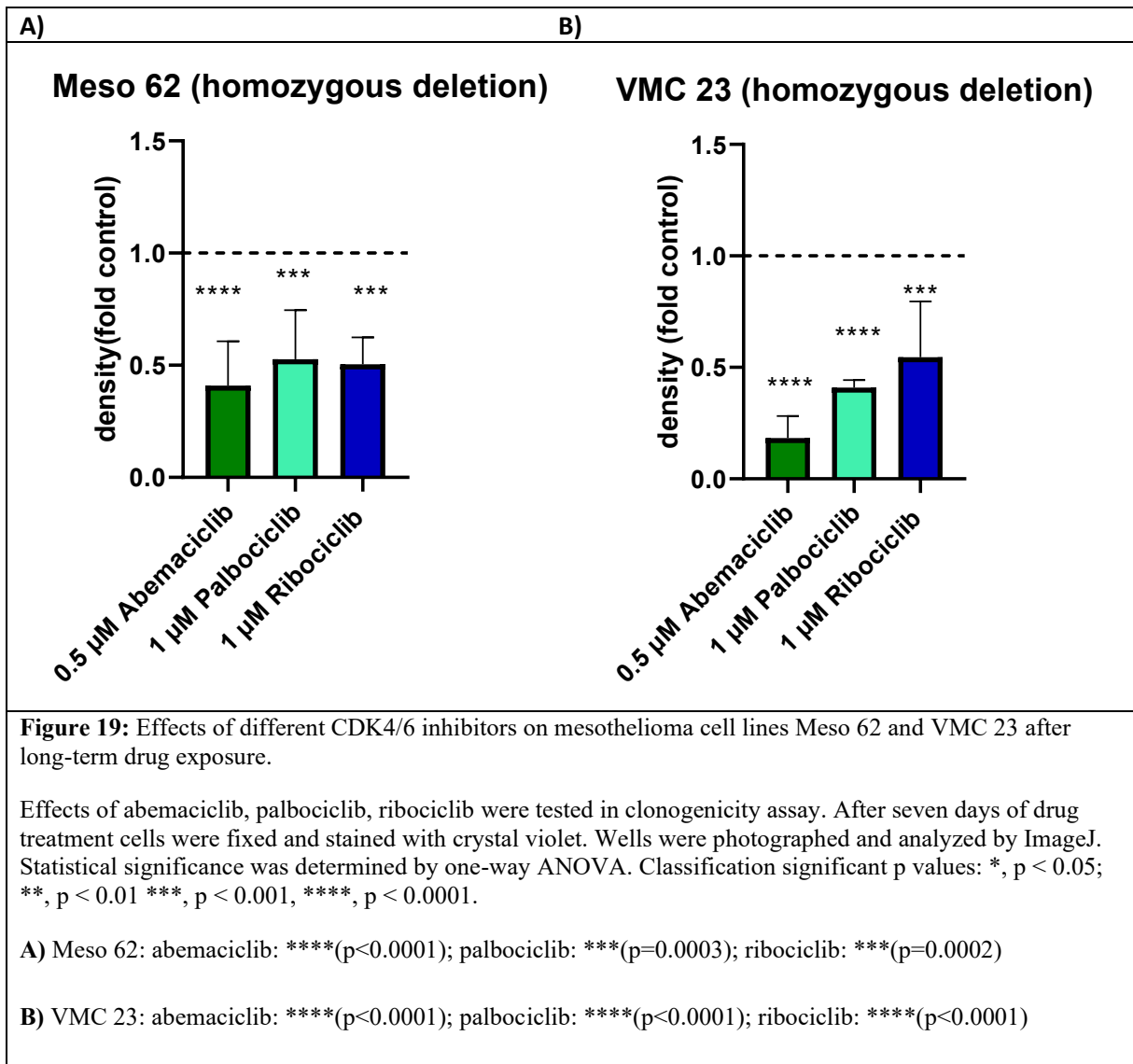




All three CDK4/6 inhibitors showed significant antiproliferative effects in both cell lines with a mutation. Already at 0.5 μM abemaciclib, cell number is reduced by almost 90 % in Meso 110 and almost completely in VMC 48 (Figure 16). This effect is also clearly visible in the pictures of the stained cells (Figure 17,18) and is consistent with the MTT assays. The

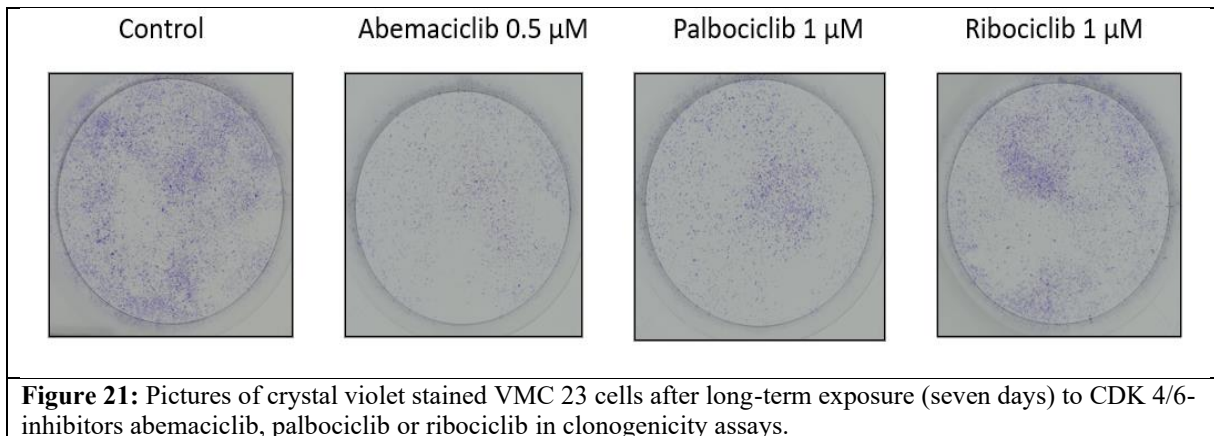
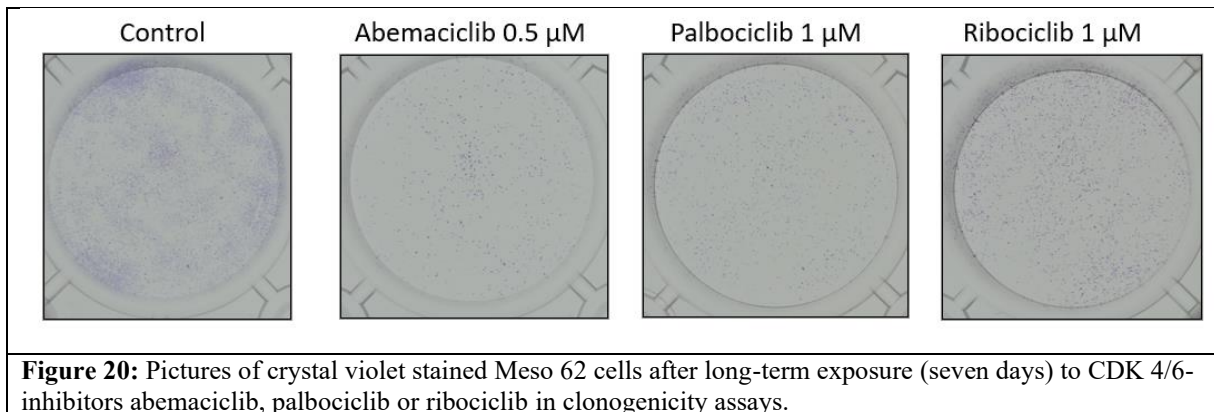
inhibitory effects of palbociclib and ribociclib increased distinctly in comparison to the MTT assays and are already detectable at 1 μM (Figure 16).





As already observed in the short-term toxicity studies, Meso 62 cells showed a weaker response to the CDK4/6 inhibitor treatment compared to the other cell lines with mutational background. Nevertheless, not only abemaciclib, but also palbociclib and ribociclib were able to achieve significant inhibitory effects (Figure 19A,20). Again, abemaciclib caused the most potent toxicity effect.

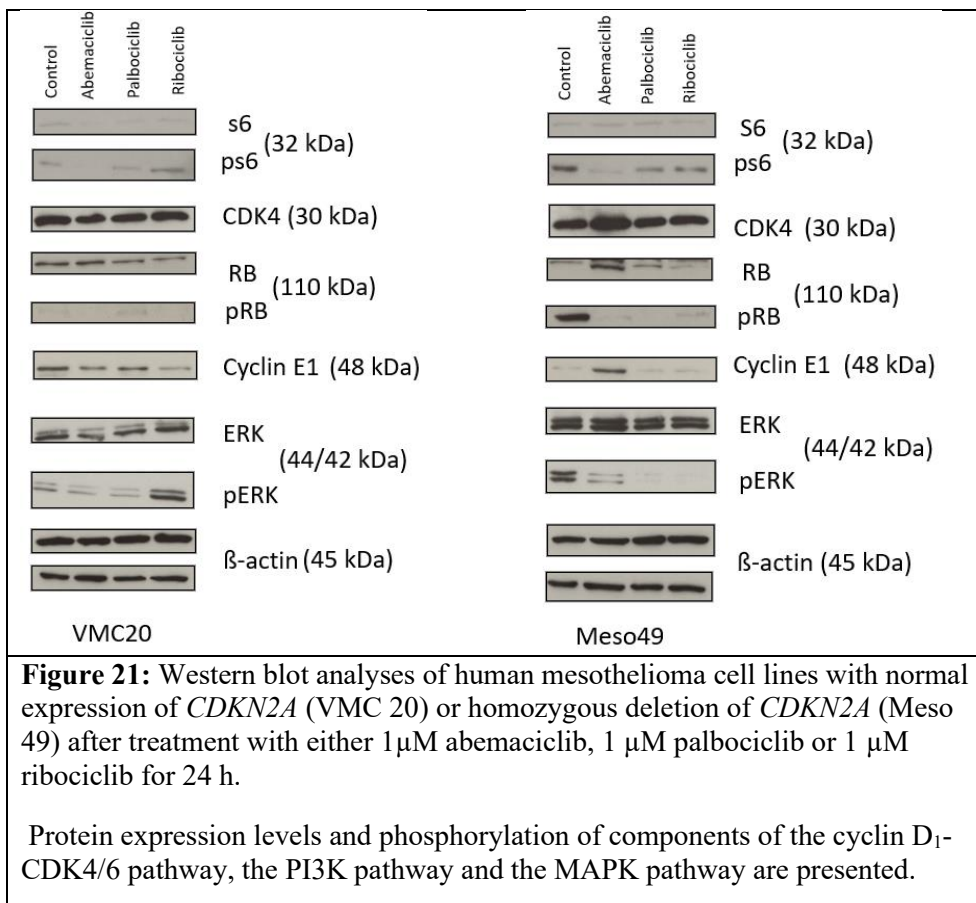
In long-term drug exposure cell viability of VMC 23 was significantly reduced by all CDK4/6 inhibitors. Just as in previous results, abemaciclib induced the strongest effect and the cell number was reduced by about 80%. (Figure 19B,21)



3.3 Impact of CDK4/6 inhibitors on downstream signaling pathways in malignant pleural mesothelioma cells:

In order to understand the impact of CDK4/6 inhibitors on protein expression of the different mesothelioma cell lines and on downstream signalling of the PI3K and the mitogen-activated protein kinase (MAPK) pathway we performed western blots (Figure 22). Cells with a normal expression of *CDKN2A* and cells with a homozygous deletion of *CDKN2A* were treated with with 1 μ M abemaciclib , 1 μ M ribociclib or 1 μ M palbociclib and proteins were isolated 24h later.

Treatment with the different CDK4/6 inhibitors caused changes in protein expression of the different cell lines.



To investigate the effects on the cyclin D₁- CDK4/6 pathway we checked the expression of CDK4, RB and pRB. In both cell lines abemaciclib inhibited phosphorylation of RB. In addition to that ribociclib seemed to inhibit phosphorylation in VMC 20 and Meso 49 and palbociclib in Meso 49. (Figure 22)

CDK4 expression levels in Meso 49 were increased under treatment with abemaciclib whereas there were no effects in VMC 20 detectable (Figure 22).

To analyze the effects of CDK4/6 inhibition on the PI3K pathway the total protein and phosphorylation levels of s6 were evaluated. Abemaciclib inhibited phosphorylation of s6 in cells with a homozygous deletion of *CDKN2A* (Meso 49) as well as in cells with a normal expression of *CDKN2A* (VMC 20, Figure 22).

The effects of the CDK4/6 inhibitors on MAPK pathway were studied by examining total and phosphorylation levels of ERK. In Meso 49 all three inhibitors showed inhibiting effects on the phosphorylation of ERK however, the expression was higher with abemaciclib than with the other inhibitors. The treatment with ribociclib seemed to increase pERK levels in VMC 20 cells. (Figure 22)

Expression of cyclin E₁ was induced by abemaciclib in cells with a homozygous deletion (Meso 49). Cyclin E₁ expression in VMC 20 was unchanged, however a slightly lower expression could be detected with ribociclib treatment. (Figure 22)

4 Discussion

4.1 Response to CDK4/6 inhibitors

Looking at the IC_{50} values for abemaciclib from the short-term toxicity assays and the results of the clonogenicity assays, our hypothesis, that human mesothelioma cell lines with a homozygous loss of *CDKN2A* show an increased sensibility to treatment with CDK4/6 inhibitors, seems to be partly confirmed. However, not only cells with a loss of *CDKN2A* showed a higher responsiveness to abemaciclib but also those with a mutation. It seemed that not only the homozygous loss of *CDKN2A* but the impaired function either through a homozygous loss or through a mutation increased sensibility of cells to CDK4/6 inhibitors.

An exception to this was the cell line Meso 62 which seemed to have a decreased sensibility to abemaciclib in short- and long-term toxicity experiments. Looking at the histotype it was recognized that it is the only cell line in our panel belonging to the sarcomatoid subtype. This subtype is more aggressive than the epithelioid and the biphasic subtypes so this could be related to the decreased sensitivity. Further experiments with cell lines from tumors of the sarcomatoid subtype could elucidate whether this subtype shows less responds to CDK4/6 inhibitors. However, Meso 62 still showed a higher sensitivity to CDK4/6 inhibitors than cell lines with a normal *CDKN2A* expression.

Furthermore, the clonogenicity assays in the cell line VMC 46 (normal expression of *CDKN2A*) also revealed unexpected results. Abemaciclib decreased cell viability in VMC 46 strongly while VMC 20 showed a lower sensitivity to the CDK4/6 inhibitors.

As the results of the two cell lines with a normal *CDKN2A* expression (VMC 20, VMC 46) were slightly contradictory long-term toxicity experiments further experiments with mesothelioma cell models without a *CDKN2A* alteration should be tested to investigate these findings in more detail.

4.2 CDK4/6 effects on protein expression

The inhibition of pRB mainly by abemaciclib but also, with a lower impact, by palbociclib and ribociclib, seen in the western blot results showed successful inhibition of the cyclin D₁-CDK4/6 pathway. When RB is hypophosphorylated by the complex, formed by CDK4/6 and cyclin D₁, it remains active. The transcription factor E2F is not released and the transcription of genes essential for G₁ to S-phase transition is impaired.

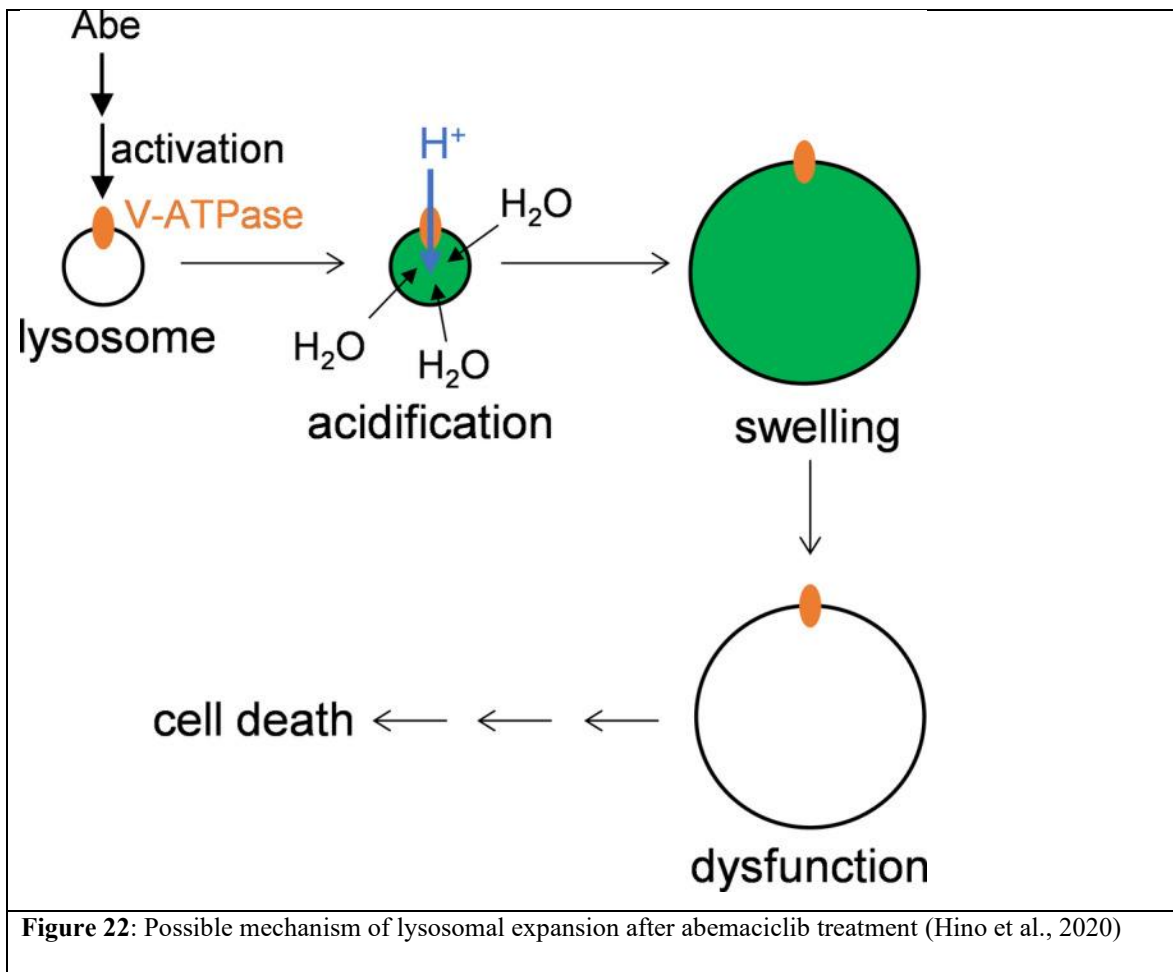
The overexpression of cyclin E₁ induced by abemaciclib treatment in cell lines with a high sensitivity to abemaciclib may indicate that the cells are trying to overcome G₁/S phase cell cycle arrest. By complexing with CDK2, cyclin E₁ is able to induce G₁ to S phase transition. The importance of cyclin E₁ overexpression in the context of resistance mechanisms to CDK4/6 inhibitors is discussed later in this thesis (Chapter 4.4.).

Both, the PI3K pathway and the MAPK pathway are crucial for cell proliferation and differentiation and therefore are involved in the cell cycle. Multiple tumours show an aberrant activity of PI3K and MAPK signaling which is known to contribute to uncontrolled cell growth and resistance to apoptosis in tumour cells .(Paraiso et al., 2010) Extracellular signal-regulated kinase (ERK) and its active form pERK is a downstream component of MAPK cascade while S6 and its active form pS6 is a downstream effector of the PI3K pathway. Both pathways were inhibited by treatment with CDK4/6 inhibitors as both, pERK and pS6, showed lower expression levels in western blots upon treatment with abemaciclib in the case of pS6 and palbociclib, ribociclib and abemaciclib in case of pERK. This suggests that treatment with CDK4/6 inhibitors was successful and induces a complete cell cycle arrest (Gelbert et al., 2014).

4.3 Mechanism of abemaciclib induced cell death

Considering the IC_{50} values and the long-term toxicity effects abemaciclib caused the most potent toxicity effect in cell lines with a mutational background. A previous study performed by Hino et al. , published in 2020 revealed that abemaciclib induces a unique form of cell death accompanied by swollen and dysfunctional lysosomes (Hino et al., 2020).

Although the mechanism is not yet fully understood, the conducted experiments suggested that abemaciclib seemed to influence vacuolar-type ATPase (V-ATPase) which serves as proton pump across the lysosomal membrane. This lead to a lysosomal acidification due to H^+ transport followed by H_2O influx into the lysosome followed by its swelling and dysfunction and finally resulted in the induction of cell death (Figure 23) (Hino et al., 2020).



Interestingly, these observations also seem plausible in the context of our experiments since the cells treated with abemaciclib showed swollen vacuoles under the microscope and impacts on cell viability of abemaciclib were significantly higher when compared to palbociclib and ribociclib in all cell lines.

In addition to that the study revealed that abemaciclib appeared to suppress, the level of phospho-mTORC1 kinase as well as its downstream effectors like pS6, through the lysosome serving as a platform for nutrient sensing and metabolic signal transduction via the mTORC1 complex (Hino et al., 2020). Considering the performed western blots (Figure 22) it becomes

clear that the expression of pS6 was inhibited by abemaciclib in comparison to the untreated cells and the cells treated with palbociclib and ribociclib. (Hino et al., 2020)

Taking into account these similar observations in the experiments, it seems possible that the increased toxicity of abemaciclib was caused by the induction of a typical cell death by dysfunctional lysosomes.

4.4 Possible resistance mechanisms

CDK4/6 inhibitors are a highly effective therapy for HR+/HER- breast cancer and our *in vitro* experiments show that they might be a promising target for treatment of MPM with mutational background of *CDKN2A*. However, acquired resistance unfortunately occurs in most cases of breast cancer patients treated with the CDK4/6 inhibitors (Gomatou et al., 2021).

A previous study revealed that cyclin E₁-CDK2 mediated phosphorylation of C-MYC can be responsible for CDK4/6 inhibitor resistance. By building a complex with CDK2, cyclin E is able to phosphorylate RB and activates proteins that are important for DNA replication. Thereby it enables entry to S phase of cell cycle. Pandey et al. noted that palbociclib-resistant HR-positive breast cancer cells had a higher cyclin E₁ expression suggesting its role in palbociclib resistance mechanisms.(Pandey et al., 2020)

Looking at the detected cyclin E₁ expression levels in the performed western blots (Figure 22), it is noted that the cell lines with a homozygous loss of *CDKN2A* showed an overexpression of cyclin E₁ upon treatment with abemaciclib in comparison to the untreated cells. In the cells with a normal expression of *CDKN2A*, which showed a lower sensitivity to the CDK4/6 inhibitors, cyclin E₁ overexpression could not be detected. The upregulation of cyclin E₁ in cells with a higher sensitivity to abemaciclib suggests that they were trying to overcome G₁/S phase arrest and may lead to CDK4/6 resistance.

In previous experiments a combined inhibition of CDK2 and CDK4/6 was able to overcome palbociclib resistance in breast cancer and leads to suppressed cell proliferation *in vitro*

(Pandey et al., 2020). Therefore, a development of a specific CDK2 inhibitor could be beneficial for the treatment of CDK4/6 resistant breast cancers as well as for other tumors like MPM that may develop CDK4/6 inhibitor resistance after treatment.

4.5 Conclusion and future perspectives

The homozygous loss of *CDKN2A* increased sensibility to CDK4/6 inhibitors, especially abemaciclib was able to achieve a very good antiproliferative effect. However, also cells with a *CDKN2A* mutation showed a good response to abemaciclib. Considering the general poor prognosis for MPM patients which is worsened by a *CDKN2A* loss of function (Markowitz et al., 2020), this treatment approach should be investigated in more detail in further experiments. Since abemaciclib achieved significantly better efficacy than palbociclib and ribociclib in all cell models, future attention could be focused on this inhibitor as a potential treatment for MPM patients with a mutation or deletion of *CDKN2A*.

However, further experiments with more cell lines need to be performed to confirm that loss of function of *CDKN2A* is truly a predictive biomarker for treatment with CDK4/6 inhibitors.

Furthermore, there is a need to clarify whether tumors with a sarcomatoid histotype generally respond worse to treatment with CDK4/6 inhibitors.

Despite the promising effects, especially with abemaciclib, possible resistance mechanisms should not remain unconsidered and should be investigated by performing resistance analyses. By detecting these possible resistance mechanisms, like overexpression of cyclin E₁, treatment with CDK 4/6 inhibitors could be even more effective through drug combinations.

5 Summary

Mesothelioma especially malignant mesothelioma is a rare tumor developing in serosal tissues like pleura und peritoneum. The most frequent type of malignant mesothelioma is malignant pleura mesothelioma (MPM) which is commonly associated with asbestos exposure. Although the usage of asbestos has been significantly reduced the incidence is still increasing due to the long latency period before tumor development (30-50 years). Prognosis of MPM is often poor related to difficult diagnosis and the absence of an effective therapy. But considering the increasing incidence and the poor prognosis for MPM patients there is an utmost need for more effective treatment strategies.

One of the most common chromosomal alteration in MPM is the loss of the tumor-suppressor gene *CDKN2A*. This gene is involved in the regulation of an important cell cycle pathway, the cyclin D₁-CDK4/6 pathway by encoding the tumor-suppressor protein p16^{INK4}. p16 inhibits CDK4/6, which stimulates cell proliferation, by binding to the Cyclin-D₁-CDK4/6 complex and leads to cell cycle arrest by blocking the phosphorylation of retinoblastoma protein (RB) and therefore the releasing of transcription factor E2F. The deletion of *CDKN2A* is the most common cause for p16 inactivation and results in a continuous activation of CDK4/6 and as consequence cell cycle progression.

This leads us to the aim of this work, to check whether homozygous deletion of *CDKN2a* in human malignant pleural mesothelioma cells lines increases their sensitivity to CDK4/6 inhibitors like abemaciclib, palbociclib and ribociclib.

To analyze toxicity effects on cell viability in MPM cell lines we performed short-term (MTT assays) and long-term (clonogenicity assays) toxicity experiments. To check the impact of treatment with CDK4/6 inhibitors on protein expression levels in the cell lines and to investigate effects on downstream signaling in PI3K and MAPK pathways, western blots were carried out.

Although further experiments have to be performed, our results suggest, that loss of function of *CDKN2A* (homozygous deletion or mutation) increases sensibility to CDK4/6 inhibitors and therefore might be a promising new treatment target for malignant pleural mesothelioma.

Das Mesotheliom, insbesondere das maligne Mesotheliom, ist ein seltener Tumor, der in serösen Geweben wie Pleura und Peritoneum entstehen. Die häufigste Form des malignen Mesothelioms ist das maligne Pleuramesotheliom (MPM), welches meistens mit Asbestexposition in Verbindung gebracht wird. Obwohl die Verwendung von Asbest deutlich zurückgegangen ist, nimmt die Inzidenz aufgrund der langen Latenzzeit vor der Tumorentwicklung (30-50 Jahre) weiterhin zu. Die Prognose von MPM ist aufgrund der schwierigen Diagnose und dem Fehlen einer wirksamen Therapie oft schlecht. Angesichts der steigenden Inzidenz und der schlechten Prognose für MPM-Patienten besteht jedoch ein dringender Bedarf an wirksameren Behandlungsstrategien.

Eine der häufigsten chromosomalen Veränderungen bei MPM ist der Verlust des Tumorsuppressorgens *CDKN2A*. Dieses Gen ist an der Regulierung eines wichtigen Zellzyklusweges, dem Cyclin-D₁-CDK4/6-Weg, beteiligt, indem es für das Tumorsuppressor Protein p16^{INK4} kodiert. p16 hemmt CDK4 und CDK6, welche die Zellproliferation stimulieren, durch Bindung an den Cyclin-D₁-CDK4/6-Komplex und führt zu einem Zellzyklusstillstand, indem es die Phosphorylierung des Retinoblastom-Proteins (RB) und damit die Freisetzung des Transkriptionsfaktors E2F blockiert. Die Deletion von *CDKN2A* ist die häufigste Ursache für die Inaktivierung von p16 und führt zu einer kontinuierlichen Aktivierung von CDK4/6 und damit zu einer Fortschreitung des Zellzyklus.

Dies führt uns zu dem Ziel dieser Arbeit, zu prüfen, ob die homozygote Deletion von *CDKN2A* in humanen malignen Pleuramesotheliom-Zelllinien deren Empfindlichkeit gegenüber CDK4/6-Inhibitoren wie Abemaciclib, Palbociclib und Ribociclib erhöht. Zur Analyse der Toxizitätseffekte auf die Zell Viabilität von MPM-Zelllinien führten wir Kurzzeit- und Langzeit-Toxizitätsexperimente durch. Um die Effekte der Behandlung mit CDK4/6-Inhibitoren auf die Proteinexpression in den Zelllinien zu prüfen und die Auswirkungen auf die Signalwege PI3K und MAPK zu untersuchen, wurden Western Blots durchgeführt.

Obwohl noch weitere Experimente durchgeführt werden müssen, deuten unsere Ergebnisse darauf hin, dass der Funktionsverlust von *CDKN2A* (homozygote Deletion oder Mutation) die Empfindlichkeit gegenüber CDK4/6-Inhibitoren erhöht und daher ein vielversprechendes neues Behandlungsziel für maligne Pleuramesotheliome darstellen könnte.

6 List of abbreviations

Abbreviation	Explanation
AKT	Protein kinase B
ANOVA	Analysis of variance
APS	Ammonium persulfate
BSA	bovine serum albumin
<i>BAP1</i>	BRCA1-associated protein 1
BCA	Bicinchoninic acid
CDK	Cyclin-dependent kinase
CAK	CDK-activating kinase
DMSO	Dimethyl Sulfoxide
E2F	E2 factor
ERK	Extracellular signal-regulated kinases
EPP	Extrapleural pneumonectomy
HCL	Hydrochloride
HER2-	Human epidermal growth factor receptor 2 negative
HR+	Hormone receptor-positive
FBS	Fetal bovine serum
MAPK	Mitogen-activated protein kinase
MPM	Malignant pleural mesothelioma
<i>NF2</i>	Neurofibromatosis type 2
p16	Cyclin-dependent kinase inhibitor 2A
PBS	Phosphate buffered saline
P/D	Pleurectomy/decortication
PI3K	Phosphoinositide 3-kinase
PMSF	Phenylmethylsulfonyl fluoride
PVDF	Polyvinylidenfluorid
RB	Retinoblastoma protein
SDS	Sodium dodecyl sulfate
TBST	Tris-buffered saline with Tween20
TEMED	Tetramethyl ethylenediamine

7 Bibliography

- Alberts, B. (2017). *Molecular Biology of the Cell*. W.W. Norton.
<https://books.google.at/books?id=2xIwDwAAQBAJ>
- Ammazzalorso, A., & Agamennone, M. (2021). *Development of CDK4 / 6 Inhibitors : A Five Years Update. Figure 1*.
- Berzenji, L., & Van Schil, P. (2018). Multimodality treatment of malignant pleural mesothelioma [version 1; peer review: 2 approved]. *F1000Research*, 7(0), 1–8.
<https://doi.org/10.12688/F1000RESEARCH.15796.1>
- Bibby, A. C., Tsim, S., Kanellakis, N., Ball, H., Talbot, D. C., Blyth, K. G., Maskell, N. A., & Psallidas, I. (2016). Malignant pleural mesothelioma: An update on investigation, diagnosis and treatment. *European Respiratory Review*, 25(142), 472–486.
<https://doi.org/10.1183/16000617.0063-2016>
- Cakiroglu, E., & Senturk, S. (2020). Genomics and functional genomics of malignant pleural mesothelioma. *International Journal of Molecular Sciences*, 21(17), 1–37.
<https://doi.org/10.3390/ijms21176342>
- Churg, A., Galateau-Salle, F., Roden, A. C., Attanoos, R., von der Thusen, J. H., Tsao, M. S., Chang, N., De Perrot, M., & Dacic, S. (2020). Malignant mesothelioma in situ: morphologic features and clinical outcome. *Modern Pathology*, 33(2), 297–302.
<https://doi.org/10.1038/s41379-019-0347-0>
- Gelbert, L. M., Cai, S., Lin, X., Sanchez-Martinez, C., Prado, M. Del, Lallena, M. J., Torres, R., Ajamie, R. T., Wishart, G. N., Flack, R. S., Neubauer, B. L., Young, J., Chan, E. M., Iversen, P., Cronier, D., Kreklau, E., & De Dios, A. (2014). Preclinical characterization of the CDK4/6 inhibitor LY2835219: In-vivo cell cycle-dependent/independent anti-tumor activities alone/in combination with gemcitabine. *Investigational New Drugs*, 32(5), 825–837. <https://doi.org/10.1007/s10637-014-0120-7>
- Giacinti, C., & Giordano, A. (2006). RB and cell cycle progression. *Oncogene*, 25(38), 5220–5227. <https://doi.org/10.1038/sj.onc.1209615>
- Gomatou, G., Trontzas, I., Ioannou, S., Drizou, M., Syrigos, N., & Kotteas, E. (2021). Mechanisms of resistance to cyclin-dependent kinase 4 / 6 inhibitors. *Molecular Biology Reports*, 48(1), 915–925. <https://doi.org/10.1007/s11033-020-06100-3>
- Hino, H., Iriyama, N., Kokuba, H., Kazama, H., Moriya, S., Takano, N., Hiramoto, M., Aizawa, S., & Miyazawa, K. (2020). Abemaciclib induces atypical cell death in cancer cells characterized by formation of cytoplasmic vacuoles derived from lysosomes. *Cancer Science*, 111(6), 2132–2145. <https://doi.org/10.1111/cas.14419>
- Kasten, M. M., & Giordano, A. (1998). pRb and the Cdks in apoptosis and the cell cycle. In *Cell Death and Differentiation* (Vol. 5, Issue 2, pp. 132–140).
<https://doi.org/10.1038/sj.cdd.4400323>
- Lim, S., & Kaldis, P. (2013). *Cdks , cyclins and CKIs : roles beyond cell cycle regulation*. 3093, 3079–3093. <https://doi.org/10.1242/dev.091744>

- Louie, B. H., & Kurzrock, R. (2020). BAP1: Not just a BRCA1-associated protein. *Cancer Treatment Reviews*, *90*(August), 102091. <https://doi.org/10.1016/j.ctrv.2020.102091>
- Maner, B. S., Dupuis, L., Su, A., Jueng, J. J., Harding, T. P., Vii, M., Siddiqui, F. S., Hardack, M. R., Aneja, S., & Solomon, J. A. (2020). *Overview of genetic signaling pathway interactions within cutaneous malignancies*. <https://doi.org/10.20517/2394-4722.2020.60>
- Markowitz, P., Patel, M., Groisberg, R., Aisner, J., Jabbour, S. K., De, S., Ganesan, S., & Malhotra, J. (2020). Cancer Treatment and Research Communications Genomic characterization of malignant pleural mesothelioma and associated clinical outcomes. *Cancer Treatment and Research Communications*, *25*, 100232. <https://doi.org/10.1016/j.ctarc.2020.100232>
- Pandey, K., Park, N., Park, K. S., Hur, J., Cho, Y. Bin, Kang, M., An, H. J., Kim, S., Hwang, S., & Moon, Y. W. (2020). Combined cdk2 and cdk4/6 inhibition overcomes palbociclib resistance in breast cancer by enhancing senescence. *Cancers*, *12*(12), 1–17. <https://doi.org/10.3390/cancers12123566>
- Paraiso, K. H. T., Van Der Kooi, K., Messina, J. L., & Smalley, K. S. M. (2010). NIH Public Access. *Methods in Enzymology*, 549–567. <https://doi.org/10.1016/B978-0-12-381298-8.00027-7.Measurement>
- Pucci, B., Kasten, M., & Giordano, A. (2000). Cell cycle and apoptosis. *Neoplasia*, *2*(4), 291–299. <https://doi.org/10.1046/j.1365-2184.2003.00267.x>
- Robertson, K. D., & Jones, P. A. (1999). Tissue-specific alternative splicing in the human INK4a/ARF cell cycle regulatory locus. *Oncogene*, *18*(26), 3810–3820. <https://doi.org/10.1038/sj.onc.1202737>
- Sayan, M., Eren, M. F., Gupta, A., Ohri, N., Kotek, A., Babalioglu, I., Kaplan, S. O., Duran, O., Or, O. D., Cukurcayir, F., Kurtul, N., Bicakci, B. C., Kutuk, T., Senyurek, S., Turk, A., Jabbour, S. K., & Atalar, B. (2019). Current treatment strategies in malignant pleural mesothelioma with a treatment algorithm. In *Advances in Respiratory Medicine* (Vol. 87, Issue 5, pp. 289–297). <https://doi.org/10.5603/ARM.2019.0051>
- Spring, L. M., Wander, S. A., Zangardi, M., & Bardia, A. (2019). *CDK 4/6 Inhibitors in Breast Cancer: Current Controversies and Future Directions*. *21*(3), 1–14. <https://doi.org/10.1007/s11912-019-0769-3.CDK>
- Studzinski, G. P., & Danilenko, M. (2005). CHAPTER 92 - Differentiation and the Cell Cycle. In D. FELDMAN (Ed.), *Vitamin D (Second Edition)* (Second Edi, pp. 1635–1661). Academic Press. <https://doi.org/https://doi.org/10.1016/B978-012252687-9/50096-6>
- Vanarsdale, T., Boshoff, C., Arndt, K. T., & Abraham, R. T. (2015). *Molecular Pathways : Targeting the Cyclin D – CDK4 / 6 Axis for Cancer Treatment*. 2905–2911. <https://doi.org/10.1158/1078-0432.CCR-14-0816>
- Yuan, K., Wang, X., Dong, H., Min, W., Hao, H., & Yang, P. (2021). Selective inhibition of CDK4/6: A safe and effective strategy for developing anticancer drugs. *Acta Pharmaceutica Sinica B*, *11*(1), 30–54. <https://doi.org/10.1016/j.apsb.2020.05.001>

8 Tables

Table 1: Components Lysis buffer for protein extraction	12
Table 2: Components polyacrylamide gels	13
Table 3: Components sample loading buffer.....	14
Table 4: Components running buffer	14
Table 5: Components Bjerrum buffer	15
Table 6: Components 1xTBST washing solution.....	15
Table 7: Primary antibodies for western blotting.....	16
Table 8: Luminol solution for western blotting.....	17
Table 9: Average IC ₅₀ values for abemaciclib after 72 hours drug exposure in concentration of 0 – 10 μ M.....	18

9 Figures

Figure 1: The control systems of the cell cycle (Alberts, 2017)	3
Figure 2: Activation of cyclin-dependent kinases (Alberts, 2017)	4
Figure 3: The Cyclin D- CDK4/6- RB pathway (Yuan et al., 2021)	5
Figure 4: Inhibition of Cyclin D ₁ - CDK4/6- RB pathway and cell cycle progression by p16 and CDK4/6 inhibitors (Maner et al., 2020)	6
Figure 5: Structural formula abemaciclib, palbociclib and ribociclib (Ammazzalorso & Agamennone, 2021)	7
Figure 6: Effects of treatment with different CDK4/6 inhibitors in human mesothelioma cell line VMC 20 representatively shown for one experiment.	19
Figure 7: Effects of treatment with different CDK4/6 inhibitors in human mesothelioma cell line Meso 110 representatively shown for one experiment.	20
Figure 8: Effects of treatment with different CDK4/6 inhibitors in human mesothelioma cell line VMC 48 representatively shown for one experiment.	20
Figure 9: Effects of treatment with different CDK4/6 inhibitors in human mesothelioma cell line Meso 49 representatively shown for one experiment.	21
Figure 10: Effects of treatment with different CDK4/6 inhibitors in human mesothelioma cell line VMC 23 representatively shown for one experiment.	22
Figure 11: Effects of treatment with different CDK4/6 inhibitors in human mesothelioma cell line Meso 62 representatively shown for one experiment.	23
Figure 12: Effects of CDK4/6 inhibitors on human mesothelioma cell lines after long-term drug exposure.	24
Figure 13: Effects of different CDK4/6 inhibitors on mesothelioma cell lines VMC 20 and VMC 46 after long-term drug exposure.	25
Figure 14: Pictures of crystal violet stained VMC 20 after long-term exposure (seven days) to CDK 4/6- inhibitors abemaciclib, palbociclib or ribociclib in clonogenicity assay.	26
Figure 15: Pictures of crystal violet stained VMC 46 after long-term exposure (seven days) to CDK 4/6- inhibitors abemaciclib, palbociclib or ribociclib in clonogenicity assays.	26
Figure 16: Effects of different CDK4/6 inhibitors on mesothelioma cell lines Meso 110 and VMC 48 after long-term drug exposure.	27
Figure 17: Pictures of crystal violet stained Meso 110 cells after long-term exposure (seven days) to CDK 4/6- inhibitors abemaciclib, palbociclib or ribociclib in clonogenicity assays.	28
Figure 18: Pictures of crystal violet stained VMC 48 cells after long-term exposure (seven days) to CDK 4/6- inhibitors abemaciclib, palbociclib or ribociclib in clonogenicity assays.	28
Figure 19: Effects of different CDK4/6 inhibitors on mesothelioma cell lines Meso 62 and VMC 23 after long-term drug exposure.	29
Figure 20: Pictures of crystal violet stained Meso 62 cells after long-term exposure (seven days) to CDK 4/6- inhibitors abemaciclib, palbociclib or ribociclib in clonogenicity assays.	30
Figure 22: Western blot analyses of human mesothelioma cell lines with normal expression of CDKN2A (VMC 20) or homozygous deletion of CDKN2A (Meso 49) after treatment with either 1 μ M abemaciclib, 1 μ M palbociclib or 1 μ M ribociclib for 24 h.	31
Figure 23: Possible mechanism of lysosomal expansion after abemaciclib treatment (Hino et al., 2020)	36